

Relative Hydride, Proton, and Hydrogen Atom Transfer Abilities of [HM(diphosphine)₂]PF₆ Complexes (M = Pt, Ni)

Douglas E. Berning,[†] Bruce C. Noll,[‡] and Daniel L. DuBois^{*,†}

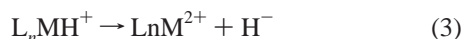
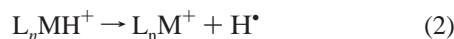
Contribution from the National Renewable Energy Laboratory, 1617 Cole Boulevard, Golden, Colorado 80401, and Department of Chemistry and Biochemistry, University of Colorado, Boulder, Colorado 80309

Received June 7, 1999

Abstract: A series of [M(diphosphine)₂]X₂, [HM(diphosphine)₂]X, and M(diphosphine)₂ complexes have been prepared for the purpose of determining the relative thermodynamic hydricities of the [HM(diphosphine)₂]X complexes (M = Ni, Pt; X = BF₄, PF₆; diphosphine = bis(diphenylphosphino)ethane (dppe), bis(diethylphosphino)ethane (depe), bis(dimethylphosphino)ethane (dmpe), bis(dimethylphosphino)propane (dmpp)). Measurements of the half-wave potentials (*E*_{1/2}) for the M(II) and M(0) complexes and p*K*_a measurements for the metal hydride complexes have been used in a thermochemical cycle to obtain quantitative thermodynamic information on the relative hydride donor abilities of the metal–hydride complexes. The hydride donor strengths vary by 23 kcal/mol and are influenced by the metal, the ligand substituents, and the size of the chelate bite of the diphosphine ligand. The best hydride donor of the complexes prepared is [HPt(dmpe)₂](PF₆), a third-row transition metal with basic substituents and a diphosphine ligand with a small chelate bite. The best hydride acceptors have the opposite characteristics. X-ray diffraction studies were carried out on eight complexes: [Ni(dmpe)₂](BF₄)₂, [Ni(depe)₂](BF₄)₂, [Ni(dmpp)₂](BF₄)₂, [Pt(dmpp)₂](PF₆)₂, [Ni(dmpe)₂](CH₃CN)](BF₄)₂, [Ni(dmpp)₂](CH₃CN)](BF₄)₂, Ni(dmpp)₂, and Pt(dmpp)₂. The cations [Ni(dmpp)₂]²⁺ and [Pt(dmpp)₂]²⁺ exhibit significant tetrahedral distortions from a square-planar geometry arising from the larger chelate bite of dmpp compared to that of dmpe. This tetrahedral distortion produces a decrease in the energy of the lowest unoccupied molecular orbital of the [M(dmpp)₂]²⁺ complexes, stabilizes the +1 oxidation state, and makes the [HM(dmpp)₂]⁺ complexes poorer hydride donors than their dmpe analogues. Another interesting structural feature is the shortening of the M–P bond upon reduction from M(II) to M(0).

Introduction

Transition-metal hydride complexes are intermediates in a variety of important stoichiometric and catalytic reactions,¹ and a knowledge of the thermodynamics associated with the formation and cleavage of the M–H bond is important to understanding known reactions and designing new ones. The M–H bond can be cleaved in three different ways, as shown in reactions 1–3. These three reactions may be regarded as half-



reactions analogous to reduction half-reactions in electrochemistry. Just as reduction potentials can be used to predict the thermodynamic driving force for an electron-transfer reaction, free energy measurements for half-reactions 1–3 can be used to determine the relative ability of metal hydrides to transfer H⁺, H[•], or H[−] in solution.

Reaction 1 is a simple deprotonation reaction, and measurements of the thermodynamics and kinetic acidity of a number of transition-metal hydrides have been reported.² The free energy scale resulting from the thermodynamic measurements is useful

in predicting quantitatively which complexes will be protonated under a given set of conditions. Whether the reactant in a catalytic cycle is a metal hydride or its deprotonated analogue can have important chemical consequences.³ The free energy scale resulting from p*K*_a measurements can be significantly extended by measuring the enthalpies of protonation reactions and making the assumption that the entropy corrections are constant for all complexes.⁴

Various approaches for measuring the free energies or enthalpies of reaction 2 as well as kinetic studies of hydrogen atom transfer reactions have been reported.^{5,6} Of particular

(2) (a) Kristjánssdóttir, S. S.; Norton, J. R. In *Transition Metal Hydrides: Recent Advances in Theory and Experiment*; Dedieu, A., Ed.; VCH: New York, 1991; pp 309–359. (b) Jordan, R. F.; Norton, J. R. *J. Am. Chem. Soc.* **1982**, *104*, 1255–1263. (c) Moore, E. J.; Sullivan, J. M.; Norton, J. R. *J. Am. Chem. Soc.* **1986**, *108*, 2257–2263. (d) Kristjánssdóttir, S. S.; Moody, A. E.; Weberg, R. T.; Norton, J. R. *Organometallics* **1988**, *7*, 1983–1987. (e) Jessop, P. G.; Morris, R. H. *Coord. Chem. Rev.* **1992**, *121*, 155. (f) Bullock, R. M.; Song, J.-S.; Szalda, D. J. *Organometallics* **1996**, *15*, 2504–2516. (g) Davies, S. C.; Henderson, R. A.; Hughes, D. L.; Oglieve, K. E. *J. Chem. Soc., Dalton Trans.* **1998**, 425–431.

(3) (a) Kollar, K.; Sandor, P.; Szalontai, G.; Heil, B. *J. Organomet. Chem.* **1990**, *393*, 153. (b) Takahashi, H.; Achiwa, K. *Chem. Lett.* **1987**, 1921–1922. (c) Chao, T.-H.; Espenson, J. H. *J. Am. Chem. Soc.* **1978**, *100*, 129–133.

(4) (a) Busch, R. C.; Angelici, R. J. *Inorg. Chem.* **1988**, *27*, 681–686. (b) Sowa, J. R., Jr.; Zanolli, V.; Facchin, G.; Angelici, R. J. *J. Am. Chem. Soc.* **1991**, *113*, 9185–9192. (c) Angelici, R. J. *Acc. Chem. Res.* **1995**, *28*, 51–60.

(5) (a) Simões, J. A. M.; Beauchamp, J. L. *Chem. Rev.* **1990**, *90*, 629–688. (b) Kiss, G.; Zhang, K.; Mukerjee, S. L.; Hoff, C. D. *J. Am. Chem. Soc.* **1990**, *112*, 5657–5658. (c) Schock, L. E.; Marks, T. J. *J. Am. Chem. Soc.* **1988**, *110*, 7701–7715. (d) Wei, M.; Wayland, B. B. *Organometallics* **1996**, *15*, 4681–4683.

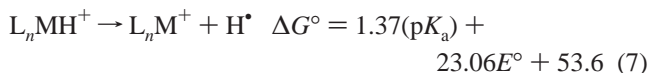
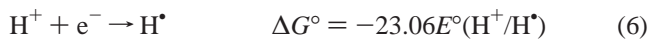
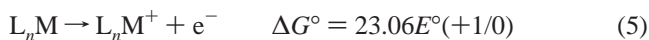
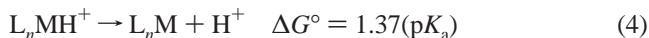
[†] National Renewable Energy Laboratory.

[‡] University of Colorado.

(1) *Transition Metal Hydrides: Recent Advances in Theory and Experiment*; Dedieu, A., Ed.; VCH: New York, 1991.

relevance to this work is the measurement of the relative free energy for the homolytic transfer of a hydrogen atom in solution, reaction 2, by means of the thermochemical cycle shown in Scheme 1, reactions 4–7.⁷ The free energy change associated

Scheme 1



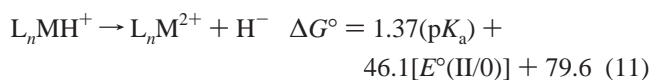
with reaction 4 can be expressed in terms of pK_a values measured in a given solvent as discussed above. The free energy associated with reaction 5 is measured by the reversible one-electron oxidation potential of M(0). Reaction 6 is the reduction of H⁺ to H[•] in the solvent of choice. The free energy associated with reaction 6 in acetonitrile has been estimated using a series of approximations,^{7a} and sources of potential errors have been discussed in the literature.^{2a,6c,8} More recent work has simply treated the free energy of this reaction as an adjustable parameter that can be determined by comparison with the enthalpy of a standard reaction and making a correction for entropy.^{7c} The result is a free energy scale that should provide a quantitative method for determining the relative hydrogen atom donor potential for a large range of compounds in solution. This scale is also useful in estimating bond dissociation enthalpies, which has been its major application. A similar thermochemical cycle has been used by Wang and Angelici to estimate bond dissociation enthalpies in solution for a large number of transition-metal hydrides.⁹ In their work, enthalpies were measured for reaction 4 and free energies for reaction 5, and the assumption was made that the entropy change for reaction 5 is negligible. Although less rigorous, this method allows compounds to be included for which it is not possible to measure pK_a values directly.

Reaction 3 is the heterolytic cleavage of the M–H bond to produce M⁺ and H[–]. The hydride transfer reaction for transition-metal hydrides is analogous to hydride transfer reactions of NADH, which are important in respiration. Hydride transfer equilibria for NADH analogues have been measured in a number of different solvents.¹⁰ The lack of similar data for transition-metal hydrides has led Dedieu to comment, “Paradoxically, much more is known about the acidic behavior of transition metal hydrides than about their hydridic behavior. In particular, the factors controlling the hydricity are far from being well-understood. There is currently no simple and unambiguous method either for identifying or for measuring the nucleophi-

licity, except for some correlation between the nucleophilic character and the position in the Periodic Table.”¹¹ To our knowledge, there has been only one previous report of *thermodynamic* measurements for this reaction for transition-metal hydrides. Sarker and Bruno have reported free energy measurements for hydride transfer between CpM(CO)₂(L)H complexes (where M = Mo, W and L = CO, PR₃) and triphenylcarbonium ion derivatives in acetonitrile.¹² The *kinetic* hydricities of various metal hydrides have been explored in a few studies. Transition-metal hydrides have been reacted with substrates such as alcohols, alkyl halides, acyl halides, aldehydes, ketones, and the trityl cation or its derivatives.¹³ Although the mechanistic pathways appear to vary depending on the metal hydride and substrate chosen for study, some general conclusions can be drawn. For isostructural complexes, those containing second- and third-row transition metals are better hydride donors than those containing first-row transition metals, and complexes with electron-donating ligands are better hydride donors than those with electron-withdrawing ligands. Also, early-transition-metal hydrides are generally more hydridic than late-transition-metal hydrides. However, as pointed out by Darensbourg and co-workers, using a different substrate as a probe of hydricity can lead to significantly different ordering of only moderately structurally diverse series of compounds.^{13c} This is not surprising if the mechanisms for these reactions are dependent on both the substrate and metal hydride chosen. A thermodynamic scale of hydricity should not be subject to this problem.

The relative free energy for hydride transfer in solution can be obtained using the thermochemical cycle shown in Scheme 2, reactions 8–11. This cycle is analogous to that used above

Scheme 2



(Scheme 1) for obtaining homolytic bond dissociation energies. The first reaction, (8), is again the measurement of the pK_a of the hydride. The second reaction, (9), is a two-electron oxidation of a M(0) complex instead of the one-electron oxidation used for obtaining homolytic bond dissociation energies. The free energy associated with this reaction may be obtained by measuring two reversible one-electron oxidations (the M/M⁺ and M⁺/M²⁺ couples) or a single reversible two-electron oxidation (the M/M²⁺ couple). The third reaction in this

(11) Dedieu, A. In *Transition Metal Hydrides: Recent Advances in Theory and Experiment*; Dedieu, A., Ed.; VCH: New York, 1991; pp 381–387.

(12) Sarker, N.; Bruno, J. W. *J. Am. Chem. Soc.* **1999**, *121*, 2174–2180.

(13) (a) Labinger, J. A. In *Transition Metal Hydrides: Recent Advances in Theory and Experiment*; Dedieu, A., Ed.; VCH: New York, 1991; pp 361–379. (b) Labinger, J. A.; Komadina, K. H. *J. Organomet. Chem.* **1978**, *155*, C25–C28. (c) Kao, S. C.; Spillett, C. T.; Ash, C.; Lusk, R.; Park, Y. K.; Darensbourg, M. Y. *Organometallics* **1985**, *4*, 83–91. (d) Kao, S. C.; Gaus, P. L.; Youngdahl, K.; Darensbourg, M. Y. *Organometallics* **1984**, *3*, 1601–1603. (e) Gaus, P. L.; Kao, S. C.; Youngdahl, K.; Darensbourg, M. Y. *J. Am. Chem. Soc.* **1985**, *107*, 2428–2434. (f) Kinney, R. J.; Jones, W. D.; Bergman, R. G. *J. Am. Chem. Soc.* **1978**, *100*, 7902–7915. (g) Martin, B. D.; Warner, K. E.; Norton, J. R. *J. Am. Chem. Soc.* **1986**, *108*, 33–39. (h) Hembre, R. T.; McQueen, J. S. *Angew. Chem., Int. Ed. Engl.* **1997**, *36*, 65–67. (i) Hembre, R. T.; McQueen, S. *J. Am. Chem. Soc.* **1994**, *116*, 2141–2142. (j) Cheng, T.-Y.; Brunschwig, B. S.; Bullock, R. M. *J. Am. Chem. Soc.* **1998**, *120*, 13121–13137.

(6) (a) Bullock, R. M.; Samsel, E. G. *J. Am. Chem. Soc.* **1990**, *112*, 6886–6898. (b) Eisenberg, D. C.; Lawrie, C. J. C.; Moody, A. E.; Norton, J. R. *J. Am. Chem. Soc.* **1991**, *113*, 4888–4895. (c) Eisenberg, D. C.; Norton, J. R. *Isr. J. Chem.* **1991**, *31*, 55–66.

(7) (a) Tilset, M.; Parker, V. D. *J. Am. Chem. Soc.* **1989**, *111*, 6711–6717. (b) Tilset, M.; Parker, V. D. *J. Am. Chem. Soc.* **1990**, *112*, 2843. (c) Parker, V. D.; Handoo, K. L.; Roness, F.; Tilset, M. *J. Am. Chem. Soc.* **1991**, *113*, 7493–7498. (d) Wayner, D. D. M.; Parker, V. D. *Acc. Chem. Res.* **1993**, *26*, 287–294.

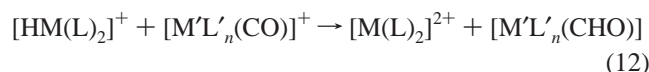
(8) Bordwell, F. G.; Harrelson, J. A., Jr.; Satish, A. V. *J. Org. Chem.* **1989**, *54*, 3101–3105.

(9) Wang, D.; Angelici, R. J. *J. Am. Chem. Soc.* **1996**, *118*, 935–942.

(10) (a) Cheng, J.-P.; Lu, Y.; Zhu, X.; Mu, L. *J. Org. Chem.* **1998**, *63*, 6108–6114. (b) Anne, A.; Moiroux, J. *J. Org. Chem.* **1990**, *55*, 4608–4614. (c) Klippenstein, J.; Arya, P.; Wayner, D. D. M. *J. Org. Chem.* **1991**, *56*, 6, 6736–6737. (d) Kreevoy, M. M.; Ostovic, D.; Lee, I.-S. H.; Binder, D. A.; King, G. W. *J. Am. Chem. Soc.* **1988**, *110*, 524–530.

thermochemical cycle, (10), is the reduction of a proton in solution by two electrons to form the hydride ion. The free energy for reaction 10 in acetonitrile is assigned a value of 79.6 kcal/mol. This value is obtained by adding the free energy of the reduction of a proton to a hydrogen atom in acetonitrile (53.6 kcal/mol in reaction 6) to that for the reduction of a hydrogen atom to H⁻ in acetonitrile. The reduction potential of a hydrogen atom in acetonitrile has been assigned a value of -1.128 V versus the ferrocene/ferrocenium couple,^{7d,14} which leads to a $\Delta G^\circ(\text{H}^+/\text{H}^-)$ value of 26.0 kcal/mol. The sources of error in determining the free energy value of 79.6 kcal/mol for reaction 10 should be similar to those encountered in determining the value of 53.6 kcal/mol for the free energy of reaction 6. Free energies of hydride transfer obtained using the cycle shown in Scheme 2 should provide a quantitative measure of the *relative* hydride donor abilities for a series of compounds in acetonitrile even if the constant of 79.6 kcal/mol is not completely accurate.

In previous work, we have shown that [HM(L)₂]⁺ complexes (where M = Ni, Pt and L is a diphosphine ligand) can transfer a hydride ligand to coordinated CO, as shown in reaction 12.¹⁵



This is an interesting reaction for several reasons. (1) Hydride transfer is occurring from a positively charged hydride complex. In other studies, hydride transfers have been observed only for anionic or neutral transition-metal hydrides. (2) These hydride donors involve late transition metals, as opposed to early transition metals for which more hydridic character is expected. (3) These metal hydride complexes can be generated by electrochemical reduction of the corresponding [M(diphosphine)₂]²⁺ complexes in the presence of a proton source. In this respect, these [HM(diphosphine)₂]⁺/[M(diphosphine)₂]²⁺ couples closely resemble NADH/NAD⁺ couples in biological systems. (4) A carbonyl ligand is reduced to a formyl ligand, a reaction that generally requires a main-group-metal hydride as the reductant,¹⁶ although a few transition-metal hydride donors are known for this reaction.¹⁷ (5) The ability of reaction 12 to proceed as shown is strongly dependent on the nature of both the hydride donor complexes and the carbonyl complexes. (6) The [M(diphosphine)₂]²⁺ complexes undergo either two one-electron reductions or a single two-electron reduction. This suggests that if pK_a measurements can be made for the [HM(diphosphine)₂]⁺ complexes, a quantitative thermodynamic scale of relative hydride donor abilities could be made for these complexes using the thermochemical cycle outlined above. In this paper, we describe such measurements and examine how

(14) Zhang, X.-M.; Bruno, J. W.; Enyinnaya, E. *J. Org. Chem.* **1998**, *63*, 4671–4678.

(15) Miedaner, A.; DuBois, D. L.; Curtis, C. J.; Haltiwanger, R. C. *Organometallics* **1993**, *12*, 299–303.

(16) (a) Casey, C. P.; Andrews, M. A.; McAlister, D. R.; Rinz, J. E. *J. Am. Chem. Soc.* **1980**, *102*, 1927. (b) Sweet, J. R.; Graham, W. A. G. *J. Am. Chem. Soc.* **1982**, *104*, 2811. (c) Tam, W.; Lin, G.-Y.; Wong, W.-K.; Kiel, W. A.; Wong, V. K.; Gladysz, J. A. *J. Am. Chem. Soc.* **1982**, *104*, 141.

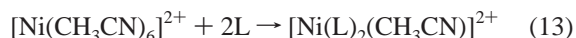
(17) (a) Wolcanski, P. T.; Bercaw, J. E. *Acc. Chem. Res.* **1980**, *13*, 121. (b) Labinger, J. A.; Wong, K. A.; Sheidt, W. R. *J. Am. Chem. Soc.* **1978**, *100*, 3254. (c) Fagan, P.; Moloy, K.; Marks, T. J. *J. Am. Chem. Soc.* **1981**, *103*, 6959. (d) Nelson, G. O.; Sumner, C. E. *Organometallics* **1986**, *5*, 1983. (e) Farnos, M. D.; Woods, B. A.; Wayland, B. B. *J. Am. Chem. Soc.* **1986**, *108*, 3659. (f) Zhang, X.-X.; Parks, G. F.; Wayland, B. B. *J. Am. Chem. Soc.* **1997**, *119*, 7938–7944. (g) Dombek, B. D. *Organometallics* **1985**, *4*, 1707. (h) Darensbourg, M. Y.; Ash, C. E.; Arndt, L. W.; Janzen, C. P.; Youngdahl, K. A.; Park, Y. K. *J. Organomet. Chem.* **1990**, *383*, 191.

various parameters influence the ability of [HM(diphosphine)₂]⁺ to function as hydride donors.

Results

Synthesis and Spectral Characterization of Complexes. Ni(II), Ni(0), Ni–H, Pt(II), Pt(0), and Pt–H complexes were prepared to probe the relationship between first- and third-row transition-metal complexes as hydride donors. In some cases, Pd(II) and Pd(0) complexes were prepared as well, but as discussed below we were unable to synthesize the corresponding palladium hydride complexes. Four diphosphine ligands—1,2-bis(dimethylphosphino)ethane (dmpe), 1,2-bis(diethylphosphino)ethane (depe), 1,2-bis(diphenylphosphino)ethane (dppe), and 1,3-bis(dimethylphosphino)propane (dmpp)—were studied for both the Ni and Pt complexes. Three different phosphine substituents, methyl, ethyl, and phenyl, are used to probe the electron-donating effect of substituents, whereas dmpe and dmpp are used to probe the effect of chelate bite size. In some instances, other ligands were used to complement these four.

The reaction of [Ni(CH₃CN)₆](BF₄)₂ with the appropriate diphosphine ligand produces five-coordinate [Ni(diphosphine)₂-(CH₃CN)](BF₄)₂ complexes, as shown in reaction 13. Two



infrared bands are observed for [Ni(dmpe)₂(CH₃CN)](BF₄)₂ and [Ni(dmpp)₂(CH₃CN)](BF₄)₂ in the solid state (Nujol mulls), which are assigned to CN stretching and combination modes¹⁸ (see Table 1 for IR and ³¹P NMR data for these complexes). The acetonitrile ligand is weakly coordinated, and it can be removed to produce four-coordinate complexes by applying a vacuum or by crystallizing the complexes from a noncoordinating solvent. [Pd(diphosphine)₂](BF₄)₂ complexes and [Pt(diphosphine)₂](PF₆)₂ were prepared by similar methods (see Experimental Section), and spectral data for these complexes are also listed in Table 1.

The Ni(0) complexes, Ni(diphosphine)₂, shown in Table 1 were prepared by reacting Ni(COD)₂ with 2 equiv of the diphosphine ligand. The Pt(0) and Pd(0) complexes were prepared by reducing the corresponding Pt(II) or Pd(II) complexes with sodium naphthalenide in tetrahydrofuran (THF). These complexes are quite air sensitive, but they are thermally stable, and the complexes containing dmpe and dmpp ligands can be sublimed.

The most convenient route to the [HNi(diphosphine)₂](PF₆) complexes is to prepare the Ni(0) complexes in situ as described above and add NH₄PF₆ to protonate the metal. This method does not work for the more basic platinum analogues, because protonation of the Pt(0) derivatives with NH₄PF₆ results in formation of [Pt(diphosphine)₂](PF₆)₂ and hydrogen evolution. The platinum hydrides are readily prepared by reduction of [Pt(diphosphine)₂](PF₆)₂ with NaBH₄ on alumina. Spectral data for these complexes are summarized in Table 1. The crystal structure of [HPt(depe)₂](PF₆) has been reported previously.¹⁵

Metal hydride complexes can also be prepared by reacting hydrogen gas with 1:1 mixtures of M(0) and M(II) complexes in benzonitrile. For example, [Ni(depe)₂](BF₄)₂, generated by comproportionation of Ni(depe)₂ and [Ni(depe)₂](BF₄)₂, reacts cleanly with hydrogen to form [H(Ni(depe)₂)](BF₄). Similarly, addition of hydrogen gas to a 1:1 mixture of Pt(dmpe)₂ and [Pt(dmpe)₂](PF₆)₂ results in formation of [HPt(dmpe)₂](PF₆). In

(18) Storhoff, B. N.; Lewis, C. H., Jr. *Coord. Chem. Rev.* **1977**, *33*, 1.

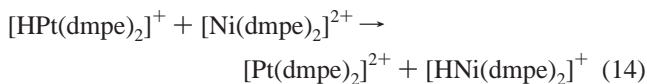
Table 1. Selected Spectral Data for M(II), M–H, and M(0) Complexes

metal	L	L'	³¹ P NMR ^a (δ)			¹ H NMR (δ) M–H (<i>J</i> _{Pt–H} , <i>J</i> _{P–H} , Hz)	IR (cm ⁻¹) ^f	
			[ML ₂]X ₂ (<i>J</i> _{Pt–P} , Hz)	[ML ₂] (<i>J</i> _{Pt–P} , Hz)	[HML ₂]X (<i>J</i> _{Pt–P} , Hz)		ν(MH)	ν(CN)
Ni	dmpe		41.8 ^c	15.0 ^b	24.6	–14.02 (8.5)	1905	2264, 2300
	depe		63.3 ^c	40.5 ^b	46.2 ^c	–14.16	1924	
	dmpp		–13.6 ^c	–19.9 ^b	–15.7 ^c	–14.33	1940	2300, 2335
	dppe		54.7 ^c		42.5 ^d	–12.87 (2.4)	1943, 1964	
Pd	dmpe		38.3 ^c	–5.3 ^b				
Pt	dmpe		35.0 (2169)	–12.6 ^b (3714)	–7.3 (2184)	–11.55 (726, 30)	2015	
	depe		58.5 (2125)	21.5 ^b (3614)	22.1 (2256)	–12.12 (650, 29)	2048	
	dmpp		–29.6 ^c (2079)	–52.1 ^b (3661)	–54.4 ^c (2295)		2072	
	dppe				20.4 ^c (2363)		2070	
	dmpe	depe		32.1 ^e (3643, 62)	32.2 ^e (2388, 72)			
				–15.9 (3665, 62)	–15.3 (2122, 72)			
	depe	dmpp		26.5 ^e (3469, 50)	38.5 ^e (2256, 66)			
				–54.6 (3765, 50)	–56.0 (2146, 66)			
	dmpe	dmpp		–9.8 ^e (3504, 55)	6.2 ^e (2551, 68)			
				–45.4 (3834, 55)	–51.3 (2142, 68)			

^a Spectra recorded in CD₃CN unless otherwise noted. ^b In toluene-*d*₈. ^c In CD₃NO₂. ^d In CD₂Cl₂. ^e In benzonitrile. ^f IR spectra were recorded as Nujol mulls. For [HNi(dppe)₂](PF₆), the two IR bands appear to arise from a solid-state effect, because only one band is observed in dichloromethane solutions.

these reactions, an equilibrium concentration of the M(I) complexes homolytically cleaves hydrogen. None of the M(diphosphine)₂ or [M(diphosphine)₂]²⁺ complexes react with hydrogen in benzonitrile. In only one case is a reaction between a M(II) species and hydrogen observed. [Ni(dmpp)₂](BF₄)₂ heterolytically cleaves hydrogen in dimethylformamide to form [HNi(dmpp)₂](BF₄) and H⁺. This reaction does not occur in benzonitrile or acetonitrile.¹⁹

Hydride Transfer Reactions. Measuring equilibrium constants for reactions of [HM(diphosphine)₂]⁺ complexes with [M'(diphosphine')₂]²⁺ complexes, as shown in reaction 14 for [HPt(dmpe)₂]⁺ and [Ni(dmpe)₂]²⁺, would be the simplest method for determining the relative hydride-donor abilities of [HM(diphosphine)₂]⁺ cations. This reaction is simply a competi-



tion between two [M(diphosphine)₂]²⁺ species for the hydride ligand, and it can be followed by ³¹P NMR spectroscopy. However, for the [HM(diphosphine)₂]⁺ and [M'(diphosphine')₂]²⁺ complexes synthesized in this study, the equilibrium constants are too large; i.e., all of the reactions are quantitative. The results obtained from these competition reactions produced a relative ordering of hydride donor abilities for these complexes of [HPt(dmpe)₂]⁺ > [HPt(depe)₂]⁺ > [HPt(dmpp)₂]⁺ > [HNi(dmpe)₂]⁺ > [HNi(depe)₂]⁺ > [HNi(dmpp)₂]⁺. Although this information is quite useful, it does not provide a quantitative measure of the driving force for these reactions.

Reactions of these six hydrides with *N*-benzylnicotinamide hexafluorophosphate, an NAD analogue, result in some hydride transfer in all cases. For [HPt(dmpe)₂]⁺, this reaction goes to completion in less than 1 h at room temperature. For [HNi(depe)₂]⁺ and [HNi(dmpp)₂]⁺, the reaction requires weeks for appreciable hydride transfer to occur. The inability of these reactions to reach equilibrium in a reasonable amount of time, coupled with a slow decomposition of the nickel hydrides under the same conditions in the absence of *N*-benzylnicotinamide hexafluorophosphate, prevented a reliable measurement of these

equilibrium constants. However, it is clear that all of the hydrides discussed in the preceding paragraph can reduce *N*-benzylnicotinamide hexafluorophosphate, which indicates that these metal hydrides are better hydride donors than *N*-benzylnicotinamide hexafluorophosphate.

pK_a Measurements. Norton and co-workers have measured the pK_a values of a number of transition-metal hydrides in acetonitrile. The choice of acetonitrile was made according to Norton for the following reasons: “(1) CH₃CN is a polar solvent (ε = 36) in which almost all hydride transition-metal complexes are soluble and in which their anions should undergo less ion pairing than in solvents such as THF; (2) CH₃CN has a low self-ionization constant (*K*_{autoprotolysis} = 3 × 10⁻²⁹) and is thus suitable for experiments over a wide range of acid and base strengths; (3) there exists a fair body of thermodynamic acid/base data for organic compounds in this solvent.”^{2b} Unfortunately, the M(diphosphine)₂ complexes which result from deprotonation of the corresponding hydrides are almost totally insoluble in acetonitrile. To overcome this solubility problem for the M(0) complexes while maintaining solvent properties similar to those of acetonitrile, we chose benzonitrile as the solvent for both pK_a and electrochemical measurements. To establish that the relative pK_a values of metal hydrides would not differ significantly between benzonitrile and acetonitrile, we measured the equilibrium constants for the reactions of [HNi(dppe)₂]⁺ with pyridine and [HPt(dppe)₂]⁺ with triethylamine in both acetonitrile and benzonitrile by ³¹P NMR spectroscopy. Using a pK_a value of 12.3 determined for pyridine in acetonitrile²⁰ for both acetonitrile and benzonitrile, we measured pK_a values of 14.2 ± 0.3 and 14.7 ± 0.3 for [HNi(dppe)₂]⁺ in acetonitrile and benzonitrile, respectively. Similarly, using a pK_a value of 18.5 determined for triethylamine in acetonitrile,²⁰ pK_a values of 22.0 ± 0.2 and 22.2 ± 0.1 were measured for [HPt(dppe)₂]⁺ in acetonitrile and benzonitrile, respectively. Thus, a ΔpK_a value (pK_a(Pt) – pK_a(Ni)) of 7.8 in acetonitrile corresponds to a ΔpK_a of 7.5 in benzonitrile. Within the accuracy of our measurements, these values are the same. On the basis of these results, we conclude that relative ΔpK_a values measured in these two solvents are not significantly different, although the absolute pK_a scales may be different.

(19) A reviewer has suggested that a cooperative action of M(0) and M(II) species in the cleavage of hydrogen is also possible. Additional experiments will be required to distinguish between these two alternatives. We would note that hydrogen is not activated by a mixture of [Pt(dmpe)₂]²⁺ and Ni(dmpe)₂.

(20) (a) Coetzee, J. F. *Prog. Phys. Org. Chem.* **1967**, *4*, 45. (b) Kolthoff, I. M.; Chantooni, M. K., Jr.; Bhowmik, S. *J. Am. Chem. Soc.* **1968**, *90*, 23–28. (c) Coetzee, J. F.; Padmanabhan, G. R. *J. Am. Chem. Soc.* **1965**, *87*, 5005.

Kristjánadóttir and Norton have proposed that the *relative* pK_a values for a series of hydrides should be the same in water, acetonitrile, and dichloromethane.^{2a}

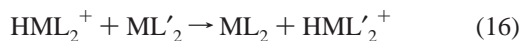
Two methods were used to measure the relative acidity of $[\text{HNi}(\text{depe})_2]^+$, $[\text{HNi}(\text{dmpp})_2]^+$, and $[\text{HNi}(\text{dmpe})_2]^+$. The first was to measure equilibrium values for reactions of the hydrides with tetramethylguanidine (TMG), as shown in reaction 15. The



$$K_{\text{eq} 15} = [\text{ML}_2][\text{TMGH}^+]/[\text{HML}_2^+][\text{TMG}]$$

M	L	$K_{\text{eq} 15}$	pK_a
Ni	depe	0.30 ± 0.13	23.8 ± 0.2
	dmpp	0.20 ± 0.15	24.0 ± 0.3
	dmpe	0.087 ± 0.04	24.4 ± 0.2
Pt	depe	$(1.6 \pm 0.8) \times 10^{-4}$	27.1 ± 0.3

$K_{\text{eq} 15}$ values are the result of five separate experiments using different ratios of reactants. The uncertainty shown is 1 standard deviation. To convert the equilibrium constants, $K_{\text{eq} 15}$, to pK_a values, the pK_a value of 23.3 for tetramethylguanidine²⁰ is added to the pK_{eq} value. The second method used for measuring the relative acidity of the nickel hydrides was to determine the equilibrium constants for the competition reactions between nickel hydride complexes and Ni(0) complexes, as shown in reaction 16. Again, five separate experiments were carried out



$$K_{\text{eq} 16} = [\text{ML}_2][\text{HML}'_2^+]/[\text{HML}_2^+][\text{ML}'_2]$$

M	L	L'	$K_{\text{eq} 16}$	$pK_a(\text{HML}'_2^+)$
Ni	depe	dmpp	1.27 ± 0.2	23.9
	depe	dmpe	3.40 ± 0.5	24.3
	dmpp	dmpe	2.41 ± 0.2	
Pt	depe	dmpp	5.16 ± 0.5	27.8
	depe	dmpe	27.6 ± 6	28.5
	dmpp	dmpe	5.62 ± 0.4	

using different stoichiometric ratios of the reactants. To ensure that equilibrium was being obtained, measurements of K_{eq} were made starting from opposite sides of the equilibrium. For example, $K_{\text{eq} 16}$ was determined both for the reaction of $[\text{HNi}(\text{depe})_2]^+$ with $\text{Ni}(\text{dmpe})_2$ and for the reverse reaction of $\text{Ni}(\text{depe})_2$ with $[\text{HNi}(\text{dmpe})_2]^+$. The pK_a values for $[\text{HNi}(\text{dmpe})_2]^+$ and $[\text{HNi}(\text{dmpp})_2]^+$ were then calculated by adding 23.8 (obtained from reaction 15) to $\log K_{\text{eq} 16}$ for the reactions of $[\text{Ni}(\text{dmpp})_2]$ and $[\text{Ni}(\text{dmpe})_2]$ with $[\text{HNi}(\text{depe})_2]^+$. The pK_a values for $[\text{HNi}(\text{dmpp})_2]^+$ and $[\text{HNi}(\text{dmpe})_2]^+$ calculated using this approach are in good agreement with those determined by direct reaction with TMG (reaction 15). The relative pK_a values resulting from competition reactions between two different metal complexes are more accurate than those resulting from reaction 15, because all of the species in reaction 16 are spectroscopically observable in the same experiment. The temperature dependence of equilibrium 16 has been studied by ^{31}P NMR for the reactions of $[\text{HNi}(\text{dmpp})_2]^+$ with $\text{Ni}(\text{dmpe})_2$, of $[\text{HNi}(\text{dmpp})_2]^+$ with $\text{Ni}(\text{depe})_2$, and of $[\text{HNi}(\text{depe})_2]^+$ with $\text{Ni}(\text{dmpe})_2$. Plots of ΔG° versus T give ΔS° values of 6 ± 2 , 5 ± 2 , and -4 ± 2 cal/(K mol), respectively, for these three reactions. These values indicate the entropy changes associated with these proton exchange reactions are small.

The pK_a of tetramethylguanidine is not large enough for it to deprotonate all of the $[\text{HPt}(\text{diphosphine})_2]^+$ complexes at reasonable concentrations. When the equilibrium constant was

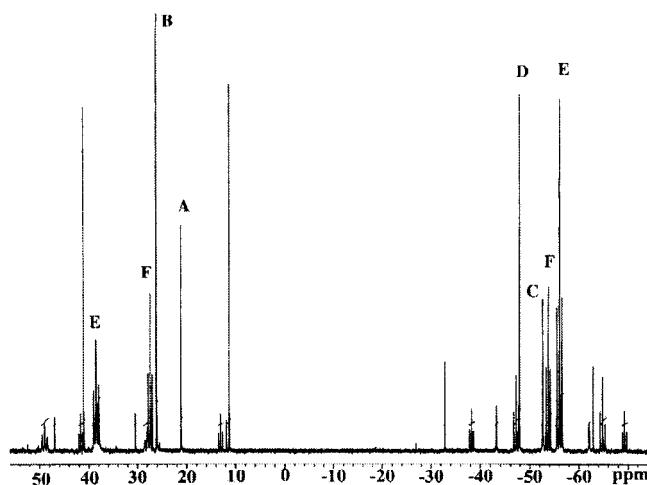
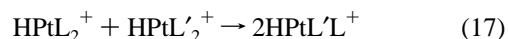


Figure 1. ^{31}P NMR spectrum of the reaction of $[\text{Pt}(\text{depe})_2\text{H}]\text{PF}_6$ and $\text{Pt}(\text{dmpp})_2$ in benzonitrile. The ^{195}Pt satellites have not been labeled for clarity. The labels are as follows: (A) $[\text{Pt}(\text{depe})_2\text{H}]\text{PF}_6$; (B) $\text{Pt}(\text{depe})_2$; (C) $[\text{HPt}(\text{dmpp})_2]\text{PF}_6$; (D) $\text{Pt}(\text{dmpp})_2$; (E) $[\text{HPt}(\text{depe})(\text{dmpp})]\text{PF}_6$; (F) $\text{Pt}(\text{depe})(\text{dmpp})$. The spectrum has been enlarged to facilitate the viewing of the smaller peaks, and the top portion of peak B which corresponds to $\text{Pt}(\text{depe})_2$ has been cropped.

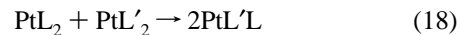
measured for the reaction of $[\text{HPt}(\text{depe})_2]^+$ with a large excess of tetramethylguanidine, a pK_a value for this complex of 27.1 could be established (reaction 15, last entry). The equilibrium constants for the reaction of $[\text{HPt}(\text{depe})_2]^+$ with $\text{Pt}(\text{dmpe})_2$ and $\text{Pt}(\text{dmpp})_2$ were then used to calculate the pK_a values for the last two complexes. Using this approach, the pK_a values for the six hydrides shown in reactions 15 and 16 are all referenced to TMG.

For the Pt complexes, there is an exchange of the diphosphine ligands to produce $[\text{HPt}(\text{L})(\text{L}')]^+$ and $\text{Pt}(\text{L})(\text{L}')$, which accompanies the proton exchange reaction, 16. That is, equilibria 17 and 18 also occur. This results in fairly complex ^{31}P NMR



$$K_{\text{eq} 17} = [\text{HPtLL}'^+]^2/[\text{HPtL}_2^+][\text{HPtL}'_2^+]$$

L	L'	$K_{\text{eq} 17}$
depe	dmpp	27.6 ± 2.7 (30.8 ± 1.9)
depe	dmpe	16.7 ± 1.1 (17.2 ± 3.6)
dmpp	dmpe	39.9 ± 3.5 (38.1 ± 2.3)



$$K_{\text{eq} 18} = [\text{PtLL}']^2/[\text{PtL}_2][\text{PtL}'_2]$$

L	L'	$K_{\text{eq} 18}$
depe	dmpp	2.36 ± 0.02 (2.30 ± 0.12)
depe	dmpe	21.3 ± 1.2 (26.3 ± 2.4)
dmpp	dmpe	13.9 ± 0.3 (14.0 ± 0.8)

spectra, as shown in Figure 1 for the reaction of $[\text{HPt}(\text{depe})_2]^+$ with $\text{Pt}(\text{dmpp})_2$. Because of equilibria 17 and 18, all three possible hydride species ($[\text{HPt}(\text{depe})_2]^+$, $[\text{HPt}(\text{dmpp})_2]^+$, and $[\text{HPt}(\text{depe})(\text{dmpp})]^+$) and all three possible Pt(0) species ($\text{Pt}(\text{depe})_2$, $\text{Pt}(\text{dmpp})_2$, and $\text{Pt}(\text{depe})(\text{dmpp})$) are present. In Figure 1, the four singlets (A–D) with their associated Pt satellites are assigned to two Pt(0) and two platinum hydride species containing two identical diphosphine ligands. The two mixed species each have A_2X_2 spin systems that appear as two triplets with associated Pt satellites. The resonances with negative chemical shift values (approximately -55 ppm) in Figure 1 are

assigned to the dmpp ligand in [HPt(depe)(dmpp)]⁺ and Pt(depe)(dmpp), because the chemical shifts are similar to those of [HPt(dmpp)₂]⁺ and Pt(dmpp)₂ (see Table 1). The resonances with positive chemical shifts (approximately +30 ppm) are assigned to the coordinated depe ligand of [HPt(depe)(dmpp)]⁺ and Pt(depe)(dmpp) on the basis of the similarity of their chemical shifts with those of [HPt(depe)₂]⁺ and Pt(depe)₂. The large chemical shift difference between diphosphine ligands in five- and six-membered chelate rings (approximately 80 ppm) is well-documented.²¹ Two criteria were used to assign the triplet resonances to either the mixed platinum hydride or the mixed Pt(0) species. First, for the unmixed complexes, ¹J_{Pt-P} is larger for the Pt(0) complexes (approximately 3600–3700 Hz) than for the platinum hydride complexes (approximately 2200–2300 Hz), as can be seen from Table 1. This should be true for the mixed-ligand complexes as well. Second, the chemical shifts for the unmixed hydride complexes are negative of the chemical shifts of their corresponding Pt(0) analogues; therefore, it is expected that the triplet resonances of [HPt(depe)(dmpp)]⁺ will occur at more negative chemical shifts than for the triplet resonances of [Pt(depe)(dmpp)]. These assignments were confirmed by ³¹P NMR spectra recorded on reactions between the various hydride complexes, reaction 17, which produce only mixed hydride species. Similarly, reaction 18 produces only mixed Pt(0) complexes. Equilibrium constants for reactions 17 and 18 were calculated from ³¹P NMR data for reactions 17 and 18, and from reaction 16 (values in parentheses for K_{eq 17} and K_{eq 18}). Both equilibria 17 and 18 are reached rapidly (in 45 min or less) for the Pt complexes, but significant concentrations of the mixed-ligand species are not observed for the Ni complexes at room temperature. In addition, no significant exchange of diphosphine ligands is observed for either [Ni(diphosphine)₂]²⁺ or [Pt(diphosphine)₂]²⁺ complexes on the basis of ³¹P NMR studies of mixtures of [M(L)₂]²⁺ and [M(L')₂]²⁺ complexes.

As can be seen from Figure 1, although the spectra are complex, the reactions interconverting the six species involved are clean. There are no significant unassigned peaks observed in the ³¹P NMR spectra for these reactions. Using the integration ratios obtained from such spectra, it is possible to measure equilibrium constants for the proton transfer between mixed and unmixed ligand complexes as shown in reaction 19. These



$$K_{\text{eq 19}} = \frac{[\text{HPtL'L}^+][\text{PtL}_2]}{[\text{HPtL}_2^+][\text{PtL'L}]}$$

L	L'	K _{eq 19}	pK _a (HML'L ⁺)
depe	dmpp	8.31 ± 0.20	28.1
depe	dmpe	3.60 ± 1.65	27.8
dmpp	dmpe	3.77 ± 0.30	28.5

equilibrium constants can then be used to calculate pK_a values for the mixed-ligand complexes in the same way as they were calculated for the unmixed complexes using reaction 16. Combining these results with the equilibrium studies described above provides pK_a values for 11 different [HM(diphosphine)₂]⁺ complexes.

To determine if pK_a data could be obtained for a Pd–H complex, a solution of Pd(dmpp)₂ in benzonitrile was mixed with a solution of [HPt(dmpp)₂]⁺, but no reaction was observed. A similar experiment with [HNi(dmpp)₂]⁺ resulted in the formation of [Pd(dmpp)₂]²⁺ and Ni(dmpp)₂ in a 1:2 ratio,

(21) Garrou, P. E. *Chem. Rev.* **1981**, *81*, 229.

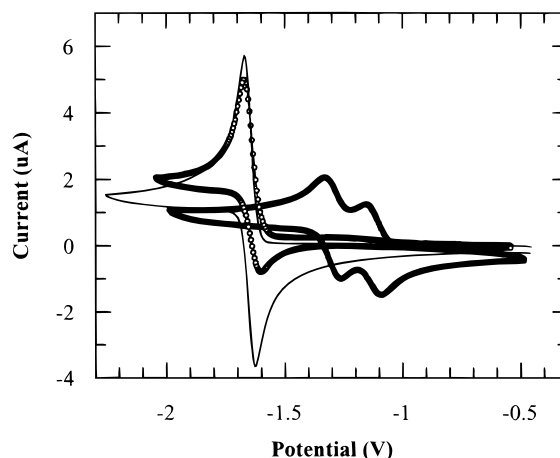
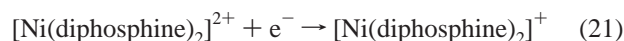
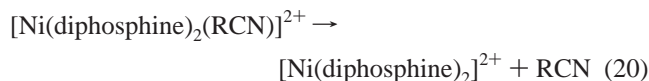


Figure 2. Cyclic voltammograms of 1×10^{-3} M solutions of (a, thin solid line) [Pt(depe)₂]₂[PF₆]₂ in acetonitrile; (b, line with open circles) [Pt(depe)₂]₂[PF₆]₂ in benzonitrile; (c, thick solid line) [Ni(depe)₂]₂[BF₄]₂ in benzonitrile. The scan rate was 0.05 V/s, and the working electrode was a 2 mm diameter glassy-carbon electrode. The potentials are referenced to the ferrocene/ferrocenium couple.

presumably with the formation of H₂. Although these experiments do not provide the data needed for an accurate pK_a value, they suggest a value between 23.9 and 27.8. These experiments also indicate that Pd hydrides are less stable to protonation than their nickel and platinum analogues (i.e., the pH range over which they are stable must be small).

Electrochemical Measurements. Cyclic voltammograms of [Ni(depe)₂]²⁺ in benzonitrile and [Pt(depe)₂]²⁺ in benzonitrile and acetonitrile are shown in Figure 2. It can be seen that [Ni(depe)₂]²⁺ undergoes two reversible one-electron reductions, which is typical for the nickel complexes.^{22a} The half-wave potentials, E_{1/2}, of the nickel complexes shown in Table 2 have an estimated accuracy of ±0.02 V. Controlled-potential electrolysis of [Ni(dmpp)₂]²⁺ at −0.96 V resulted in the passage of 0.8 faraday of charge/mol of complex, consistent with a one-electron reduction. Plots of the peak current vs the square root of the scan rate are linear for both of the reduction waves of the Ni complexes for scan rates between 0.05 and 4.0 V/s, indicating diffusion-controlled reductions.

On the basis of the structural and spectroscopic results, the Ni(II) complexes can exist as either four- or five-coordinate species, as shown in equilibrium 20. Recrystallization of the



complexes in the absence of added acetonitrile or benzonitrile results in four-coordinate species, indicating that the equilibrium lies to the right under these conditions. However, recrystallization in the presence of benzonitrile or acetonitrile results in the formation of five-coordinate species. As one might expect, the net result of equilibrium 20 is to shift the reduction potential for the Ni(II/I) couple (reaction 21) to more negative potentials as the concentration of acetonitrile or benzonitrile increases. This is caused by a decrease in the concentration of the more easily reduced four-coordinate [Ni(diphosphine)₂]²⁺ species. The E_{1/2} values for the Ni(II/I) couples shift by −0.04 to −0.11 V

(22) (a) Miedaner, A.; Haltiwanger, R. C.; DuBois, D. L. *Inorg. Chem.* **1991**, *30*, 417–427. (b) Alyea, C. E.; Meek, D. W. *Inorg. Chem.* **1972**, *11*, 1029.

Table 2. Electrochemical Data for M(diphosphine)₂ Complexes

compd	$E_{1/2}(\text{II/I})^a$ (V)	$E_{1/2}(\text{I/O})^a$ (V)	$E_{1/2}(\text{II/O})^a$ (V)	$\Delta G^{\circ}_{22}^b$ (kcal/mol)	ΔS°_{22} (cal/(K mol))	ΔH°_{22} (kcal/mol)	$\Delta S^{\circ}_{\text{rc}}(\text{I/O})$ (cal/(K mol))		$\Delta S^{\circ}_{\text{rc}}(\text{II/I})$ (cal/(K mol))		$\Delta S^{\circ}_{\text{rc}}(\text{II/O})$ (cal/(K mol))	
							exptl ^c	calcd ^d	exptl ^c	calcd ^d	exptl ^c	calcd ^d
Ni(dppp) ₂	(-0.19)	(-0.91)		25.4								
Ni(dppe) ₂	[-0.12]	[-0.95]		36.9	11	40.1	6.7	16	30.5	22	37.2	38
	-0.70	-0.90										
Ni(dmpp) ₂	(-0.70)	(-0.88)		50.2	27.3	58.2	15.8	18	37.7	28	53.5	46
	[-0.66]	[-0.95]										
	-0.86	-1.32										
Ni(depe) ₂	(-0.89)	(-1.33)		56.0	23.7	63.0	12.2	18	37.7	28	49.9	46
	[-0.76]	[-1.35]										
	-1.13	-1.30										
Pt(dppe) ₂	(-1.16)	(-1.29)		57.2	20.5	64.6					46.7	38
	[-1.04]	[-1.34]										
Ni(dmpe) ₂			-1.24	62.3	29.5	71.0					55.7	46
			(-1.39)									
Pt(dmpp) ₂			[-1.32]	69.6	14.7	73.9					40.9	46
			(-1.53)									
Pt(depe) ₂			-1.63	75.2	22.9	81.9					49.1	46
			(-1.65)									
Pt(dmpe) ₂			-1.73	79.8	41	91.8					67	46

^a Half-wave potentials vs FeCp₂ for the II/I, I/O, and II/O couples in benzonitrile; potentials in acetonitrile are given in parentheses, and those in dichloromethane or dichloroethane are given in brackets. ^b Free energy for reaction 22 in benzonitrile calculated from $\Delta G^{\circ} = -nFE^{\circ}$ assuming $E^{\circ} = \frac{1}{2}[E_{1/2}(\text{II/I}) + E_{1/2}(\text{I/O})]$ and $n = 2$. ^c Entropy changes associated with II/I, I/O, and II/O redox couples in benzonitrile; entropy changes in acetonitrile are given in parentheses. ^d Calculated values were obtained by using eq 24 with AN values of 15.5 for benzonitrile and 19.3 for acetonitrile and r values of 4.0 and 7.0 for complexes with methyl and phenyl substituents, respectively.

upon changing from noncoordinating solvents, such as dichloroethane or dichloromethane (shown by the values in brackets in Table 2), to pure benzonitrile or acetonitrile (values in parentheses in Table 2). These shifts correspond to free energy changes of 0.9–2.5 kcal/mol or to equilibrium constants for reaction 20 between 0.2 and 5 at room temperature.²³ Titration of a dichloroethane solution of [Ni(dmpp)₂](BF₄)₂ with acetonitrile was followed by UV–visible spectroscopy to determine an equilibrium constant of 0.8 for reaction 20.²⁴ These values are consistent with spectroscopic measurements, which indicate that the acetonitrile ligands of the five-coordinate [Ni(diphosphine)₂(CH₃CN)]²⁺ species are fully dissociated in noncoordinating solvents.

[Pt(depe)₂]²⁺ undergoes a quasi-reversible ($\Delta E_p = 68$ mV at 50 mV/s) two-electron reduction in benzonitrile and a nearly reversible two-electron reduction in acetonitrile ($\Delta E_p = 46$ mV at 50 mV/s). A comparison of the slopes of the chronoamperometric plots for potential steps across the reduction wave of [Pt(depe)₂]²⁺ and the two reduction waves of [Ni(dmpp)₂]²⁺ in benzonitrile gives a ratio of 1.1:1.0. Because the slopes are proportional to the number of electrons involved in the charge transfer, these results are consistent with a two-electron reduction of [Pt(depe)₂]²⁺. Pt(dmpp)₂ and Pt(dmpe)₂ exhibit quasi-reversible oxidations in benzonitrile with peak-to-peak separations of 106 and 210 mV, respectively, at a scan rate of 10 mV/s. The failure to observe completely reversible couples for Pt(dmpp)₂ and Pt(dmpe)₂ results in larger possible errors for the $E_{1/2}$ values shown in Table 2 for these two complexes (estimated to be ± 0.05 V). The two-electron oxidations observed for the Pt(diphosphine)₂ complexes give $E_{1/2}$ values

that are average values for the II/I and I/O couples. No information can be obtained for the $E_{1/2}$ values of the individual II/I and I/O couples.

The temperature dependence of $E_{1/2}$ values of redox couples can provide information on the entropy changes associated with the oxidation or reduction of a species in solution. Weaver and co-workers used nonisothermal cells to obtain ΔS° values for a number of redox couples in a wide variety of solvents.²⁵ Koval and co-workers later proposed using ferrocene as a redox standard for variable-temperature measurements of the redox potentials. The measured entropy changes can then be corrected for the known entropy change of the ferrocene couple.²⁶ Equation 23 gives the relationship between the entropy change for reaction 22, E° (approximated by $E_{1/2}$), and temperature.



$$d(\Delta G^{\circ})/dT = -nFd(E^{\circ})/dT = \Delta S^{\circ}_{22} \quad (23)$$

The ΔS°_{22} values shown in Table 2 were determined by measuring the $E_{1/2}$ values as a function of temperature by differential-pulse and cyclic voltammetry. ΔG°_{22} , ΔS°_{22} , and ΔH°_{22} values for the reduction of [M(diphosphine)₂]²⁺ complexes by ferrocene at 294 K are listed in Table 2.

To obtain the experimental values for the entropy changes associated with individual redox couples ($\Delta S^{\circ}_{\text{rc}}$) of the [M(diphosphine)₂]²⁺ complexes, the entropy of the ferrocene redox couple (11.5 cal/(K mol) in acetonitrile, 13.1 cal/(K mol) in benzonitrile)²⁵ is multiplied by n (the number of electrons transferred

(23) (a) Bard, A. J.; Faulkner, L. R. *Electrochemical Methods: Fundamentals and Applications*; Wiley: New York, 1980; p 35. (b) Brown, E. R.; Large, R. F. In *Physical Methods of Chemistry Part II: Electrochemical Methods*; Weissberger, A., Rossiter, B. W., Eds.; Techniques of Chemistry I; Wiley: New York, 1971; p 483.

(24) Qualitative data for titration of [Ni(depe)₂]²⁺ in dichloromethane with acetonitrile are consistent with an equilibrium constant for this complex of approximately 1: Solar, J. M.; Ozkan, M. A.; Isci, H.; Mason, R. *Inorg. Chem.* **1984**, *23*, 758.

(25) (a) Yee, E. L.; Cave, R. J.; Guyer, K. L.; Tyma, P. D.; Weaver, M. J. *J. Am. Chem. Soc.* **1979**, *101*, 1131–1137. (b) Sahami, S.; Weaver, M. J. *J. Electroanal. Chem. Interfacial Electrochem.* **1981**, *122*, 155–170. (c) Hupp, J. T.; Weaver, M. J. *Inorg. Chem.* **1984**, *23*, 3639–3644. (d) The value of 13.1 cal/(K mol) for the entropy of the ferrocene redox couple in benzonitrile was extrapolated from Figure 6 of ref 25c using an acceptor number of 15.5.

(26) Koval, C. A.; Gustafson, R. M.; Reidsema, C. M. *Inorg. Chem.* **1987**, *26*, 950–952.

in reaction 22) and added to ΔS°_{22} . Experimental values of ΔS°_{rc} for the II/I, I/0, and II/0 couples for [M(diphosphine)₂]²⁺ complexes are also listed in Table 2. Hupp and Weaver have proposed the semiempirical relationship shown in eq 24 for calculating the entropy of a one-electron reduction.^{25c} The

$$\Delta S^\circ_{rc} = 21.9 - 0.58(\text{AN}) + 20.7(Z_{\text{ox}}^2 - Z_{\text{red}}^2)/r \quad (24)$$

acceptor number (AN) is an intrinsic property of the solvent that reflects both the electrophilicity and polarity of the solvent,²⁷ Z_{ox} and Z_{red} are the charges on the complexes in their oxidized and reduced forms, respectively, and r is the radius of the molecule in angstroms as defined by Sutin et al.²⁸ ΔS°_{rc} values calculated using this equation are listed in Table 2 following the experimental values. The values used for r are 4.0 Å for the dmpe, dmpp, and depe complexes of nickel and platinum and 7.0 Å for dppe complexes. These values are based on crystallographic data and/or molecular mechanics calculations and represent an average value expected for the II and 0 oxidation states. From eq 24 and the calculated values of ΔS°_{rc} in Table 2, it can be seen that ΔS°_{rc} for the I/0 couple is expected to be smaller than that of the II/I couple because of the larger charges involved in the latter couple. This is true where the values of ΔS°_{rc} could be obtained for both couples. The experimental ΔS°_{rc} values tend to be larger than the calculated ΔS°_{rc} values for the II/I couple. As a result, the experimental ΔS°_{rc} values are generally larger than the calculated values for the reduction from M(II) to M(0) (Table 2). Equation 24 was developed for complexes in which the ligands prevented direct interactions between the metal and solvent and for which solvent-solvent interactions were more important than solvent-metal interactions.^{25c} Because the solvent can approach and even coordinate to the metal center in the case of the Ni complexes, the agreement between the experimental and calculated values is surprising.

Thermodynamics of Hydride Transfer. The relative free energies of hydride transfer for [HM(diphosphine)₂]⁺ cations can be calculated using the thermochemical cycle shown in Scheme 2. The pK_a values for the [HM(diphosphine)₂]⁺ cations and the $E_{1/2}$ values for the II/0 couple (or the average of the II/I and I/0 couples for those complexes having two one-electron transfers) were measured for the [M(diphosphine)₂]²⁺ and M(diphosphine)₂ complexes as discussed above. $\Delta G^\circ_{\text{H}}$ values calculated according to eq 11 are listed in Table 3, along with $E_{1/2}$ values for the II/0 couples or the average of the II/I and I/0 couples. The pK_a values and $E_{1/2}$ values for the I/0 couples can also be used to determine the relative enthalpies for hydrogen atom transfer ($\Delta G^\circ_{\text{H}}$, Table 3) using Scheme 1.

Structural Studies. Crystallographic data for four four-coordinate M(II) complexes ([Ni(dmpe)₂](BF₄)₂, [Ni(depe)₂](BF₄)₂, [Ni(dmpp)₂](BF₄)₂, and [Pt(dmpp)₂](PF₆)₂), two five-coordinate Ni(II) complexes ([Ni(dmpe)₂(CH₃CN)](PF₆)₂ and [Ni(dmpp)₂(CH₃CN)](BF₄)₂), and two M(0) complexes (Ni(dmpp)₂ and Pt(dmpp)₂) are given in Table 4. Selected bond distances and bond angles are given in Tables 5 and 6, respectively. Drawings of the four four-coordinate M(II) cations are shown in Figure 3. The [Ni(dmpe)₂]²⁺ and [Ni(depe)₂]²⁺ cations are nearly planar, as measured by trans P-Ni-P angles of 178 and 180°, respectively. The dihedral angle, β , between the two planes formed by the Ni atom and the two phosphorus atoms of each bidentate ligand is 3.4° for [Ni(dmpe)₂]²⁺ and 0.0° for [Ni(depe)₂]²⁺. This angle is a useful measure of the

Table 3. Thermodynamics of Proton (pK_a), Hydrogen Atom ($\Delta H^\circ_{\text{H}}$), and Hydride ($\Delta G^\circ_{\text{H}}$) Transfer Reactions for [HM(diphosphine)₂]⁺ Complexes

M	L	pK_a	$E_{1/2}(\text{II}/0)$	$\Delta H^\circ_{\text{H}}^a$	$\Delta G^\circ_{\text{H}}^{b,c}$
Ni	dppe	14.7 ^c	-0.80	58.9	62.8
		(14.2) ^c	(-0.79)	(58.8)	(62.7)
	dmpp	23.9	-1.09	62.1	62.1
Ni	depe	23.8	(-1.11)	(61.6)	(61.2)
			-1.22	62.1	56.0
	(-1.22)	(62.4)	(56.0)		
Pt	dppe	22.2	-1.24		52.8
		(22.0)	(-1.24)		(52.5)
Ni	dmpe	24.3	-1.35	61.7	50.7
			(-1.39)	(60.8)	(48.9)
Pt	dmpp	27.8	-1.51		48.1
			(-1.53)		(47.2)
	depe	27.1	-1.63		41.6
			(-1.65)		(40.8)
dmpe	28.5	-1.73		38.8	
					(38.8)

^a Calculated using the expression $\Delta H^\circ_{\text{H}} = 1.37pK_a + 23.06E^\circ(1+0) + 59.5$.^{7c} ^b Calculated using eq 11. A value of 26.0 kcal/mol was used for ΔG° for reaction 10 in benzonitrile (the same value as for acetonitrile). Although this absolute value may not be correct for benzonitrile, the relative values calculated for $\Delta G^\circ_{\text{H}}$ should be accurate. ^c Values for benzonitrile solutions; values for acetonitrile solutions are given in parentheses.

tetrahedral distortion, which is slight for these compounds. The bite angles, P-Ni-P, of the bidentate ligands are approximately 86°, which is typical for Ni(II) complexes containing chelating phosphines with a two-carbon backbone.²² All of the Ni-P bond lengths in these two cations are close to the average value of 2.21 Å, which is in the normal range for square-planar Ni(II) compounds.²²

In contrast to [Ni(dmpe)₂]²⁺ and [Ni(depe)₂]²⁺, the [Ni(dmpp)₂]²⁺ cation exhibits a significant tetrahedral distortion. The trans P-Ni-P angles are approximately 149°, and the dihedral angle, β , between the planes defined by the two dmpp ligands and Ni is 43.7°. [Pt(dmpp)₂]²⁺ shows a smaller tetrahedral distortion, with trans P-Pt-P angles of approximately 171° and a dihedral angle β of 11.5°. The average bite angle of the dmpp ligand is 91.5° for [Ni(dmpp)₂]²⁺ and 88.3° for [Pt(dmpp)₂]²⁺. The tetrahedral distortions appear to have little effect on the M-P bond distances. For [Ni(dmpp)₂]²⁺, the average Ni-P bond distance is 2.21 Å, which is the same as that observed for the two Ni(II) complexes described above. For [Pt(dmpp)₂]²⁺, the average Pt-P bond distance is 2.33 Å, in the normal range expected for Pt(II) complexes.²⁹

The drawings shown in Figure 4 illustrate that the two five-coordinate Ni(II) complexes [Ni(dmpe)₂(CH₃CN)]²⁺ and [Ni(dmpp)₂(CH₃CN)]²⁺ have significantly different structures. [Ni(dmpe)₂(CH₃CN)]²⁺ is best described as a square-pyramidal complex with the acetonitrile ligand coordinated in the axial position, whereas [Ni(dmpp)₂(CH₃CN)]²⁺ has a trigonal-bipyramidal geometry with the acetonitrile coordinated in the equatorial position. The four N-Ni-P bond angles for [Ni(dmpe)₂(CH₃CN)]²⁺ are all within 1° of the average value of 98.4°. In contrast, the average N-Ni-P bond angle for the two axial phosphine ligands of [Ni(dmpp)₂(CH₃CN)]²⁺ is 85.1°, and the average N-Ni-P bond angle for the two equatorial phosphorus atoms is 119.1°. The average of the Ni-P bond distances for both complexes is 2.23 Å, but the two Ni-N bond distances are quite different—2.28 Å for [Ni(dmpe)₂(CH₃CN)]²⁺

(29) (a) Gieren, V. A.; Brüggeller, P.; Hofer, K.; Hübner, T.; Ruiz-Pérez, C. *Acta Crystallogr.* **1989**, C45, 196-198. (b) Brüggeller, P. *Inorg. Chem.* **1990**, 29, 1742-1750. (c) Tulip, T. H.; Yamagata, T.; Yoshida, T.; Wilson, R. D.; Ibers, J. A.; Otsuka, S. *Inorg. Chem.* **1979**, 18, 2239-2250.

(27) Gutmann, V. *Electrochim. Acta* **1976**, 21, 661-670.

(28) Brown, G. M.; Sutin, N. *J. Am. Chem. Soc.* **1979**, 101, 883-891.

Table 4. Crystallographic Data for [Ni(dmpe)₂](PF₆)₂, [Ni(depe)₂](BF₄)₂, [Ni(dmpp)₂](BF₄)₂, [Pt(dmpp)₂](PF₆)₂, [Ni(dmpe)₂(CH₃CN)](PF₆)₂, [Ni(dmpp)₂(CH₃CN)](BF₄)₂, Ni(dmpp)₂, and Pt(dmpp)₂

	[Ni(dmpe) ₂](PF ₆) ₂	[Ni(depe) ₂](BF ₄) ₂	[Ni(dmpp) ₂](BF ₄) ₂	[Pt(dmpp) ₂](PF ₆) ₂
empirical formula	C ₁₃ H ₃₅ F ₁₂ NNiO ₂ P ₆	C ₂₀ H ₅₀ B ₂ F ₈ NiOP ₄	C ₁₄ H ₃₆ B ₂ F ₈ NiP ₄	C _{15.61} H _{39.73} F ₁₂ N _{0.27} O _{0.53} P ₆ Pt
formula mass, amu	709.95	662.81	560.64	848.70
cryst syst	monoclinic	orthorhombic	monoclinic	monoclinic
space group	<i>P</i> 2 ₁ / <i>c</i>	<i>Pccn</i>	<i>P</i> 2 ₁ / <i>n</i>	<i>P</i> 2 ₁ / <i>c</i>
<i>a</i> (Å)	17.7374(2)	17.7301(2)	9.8371(13)	17.5851(17)
<i>b</i> (Å)	9.064	10.91290(10)	16.764(3)	9.3130(10)
<i>c</i> (Å)	17.9013(2)	15.77990(10)	14.8801(18)	18.412(3)
α (deg)	90	90	90	90
β (deg)	96.1870(10)	90	101.136(7)	94.269(6)
γ (deg)	90	90	90	90
<i>V</i> (Å ³)	2861.32(5)	3053.20(5)	2407.7(6)	3007.0(6)
<i>Z</i>	4	4	4	4
<i>T</i> (K)	150(2)	162(2)	160(2)	141(2)
<i>R</i> index ^a (<i>I</i> > 2σ(<i>I</i>))	R1 = 0.0315	R1 = 0.0316	R1 = 0.0286	R1 = 0.0332
<i>R</i> index ^a (all data)	R1 = 0.0434, wR2 = 0.0805	R1 = 0.0438, wR2 = 0.0731	R1 = 0.0354, wR2 = 0.0716	R1 = 0.0412, wR2 = 0.0805
weighting coeff ^b	<i>a</i> = 0.0373, <i>b</i> = 1.0395	<i>a</i> = 0.0398, <i>b</i> = 1.4490	<i>a</i> = 0.0308, <i>b</i> = 1.7342	<i>a</i> = 0.0351, <i>b</i> = 5.0718
goodness of fit ^c on <i>F</i> ²	1.047	0.914	1.034	1.047
	[Ni(dmpe) ₂ (CH ₃ CN)](PF ₆) ₂	[Ni(dmpp) ₂ (CH ₃ CN)](BF ₄) ₂	Ni(dmpp) ₂	Pt(dmpp) ₂
empirical formula	C ₁₆ H ₃₈ F ₁₂ N ₂ NiP ₆	C ₁₆ H ₃₉ B ₂ F ₈ NNiP ₄	C ₁₄ H ₃₆ NiP ₄	C ₁₄ H ₃₆ P ₄ Pt
formula mass, amu	731.01	601.69	387.02	523.40
cryst syst	monoclinic	triclinic	monoclinic	monoclinic
space group	<i>P</i> 2 ₁ / <i>c</i>	<i>P</i> $\bar{1}$	<i>C</i> 2/ <i>c</i>	<i>C</i> 2/ <i>c</i>
<i>a</i> (Å)	19.9406(4)	10.7503(12)	17.5777(17)	17.481(6)
<i>b</i> (Å)	9.0706(2)	14.2268(19)	9.5357(11)	9.892(3)
<i>c</i> (Å)	16.7066(3)	17.8531(15)	14.7122(16)	14.524(5)
α (deg)	90	93.236(6)	90	90
β (deg)	97.49	92.155(6)	123.458(5)	123.879(7)
γ (deg)	90	92.390(5)	90	90
<i>V</i> (Å ³)	2996.03(10)	2721.6(5)	2057.4(4)	2085.3(13)
<i>Z</i>	4	4	4	4
<i>T</i> (K)	170(2)	169(2)	152(2)	160(2)
<i>R</i> index ^a (<i>I</i> > 2σ(<i>I</i>))	R1 = 0.0560	R1 = 0.0528	R1 = 0.0442	R1 = 0.0218
<i>R</i> index ^a (all data)	R1 = 0.1062, wR2 = 0.1349	R1 = 0.0899, wR2 = 0.1336	R1 = 0.0638, wR2 = 0.0874	R1 = 0.0223, wR2 = 0.0510
weighting coeff ^b	<i>a</i> = 0.0313, <i>b</i> = 4.6821	<i>a</i> = 0.0482, <i>b</i> = 4.9849	<i>a</i> = 0.0227, <i>b</i> = 1.4966	<i>a</i> = 0.0308, <i>b</i> = +1/2
goodness of fit ^c on <i>F</i> ²	1.144	1.021	1.463	1.113

^a R1 = $\sum(|F_o| - |F_c|)/\sum|F_o|$; wR2 = $[\sum w(F_o^2 - F_c^2)^2/\sum w(F_o^2)^2]^{1/2}$. ^b $w^{-1} = [\sigma^2(F_o^2) + (aP)^2 + bP]$, where $P = (F_o^2 + 2F_c^2)/3$. ^c GOF = $S = [\sum w(F_o^2 - F_c^2)^2/(M - N)]^{1/2}$, where *M* is the number of reflections and *N* is the number of parameters refined.

Table 5. Selected Bond Distances (Å)

compd	M–P(1)	M–P(2)	M–P(3)	M–P(4)	M–N
[Ni(dmpe) ₂](PF ₆) ₂	2.2133(4)	2.2127(4)	2.2197(4)	2.2134(4)	
[Ni(depe) ₂](BF ₄) ₂	2.2358(3)	2.2290(4)			
[Ni(dmpp) ₂](BF ₄) ₂	2.1952(4)	2.2277(12)	2.2210(4)	2.2013(4)	
[Pt(dmpp) ₂](PF ₆) ₂	2.3042(10)	2.3080(9)	2.3243(12)	2.3178(11)	
[Ni(dmpe) ₂ (CH ₃ CN)](PF ₆) ₂	2.224(2)	2.229(2)	2.236(2)	2.225(2)	2.278(19)
[Ni(dmpp) ₂ (CH ₃ CN)](BF ₄) ₂	2.2120(11)	2.2131(11)	2.2206(12)	2.2617(11)	1.992(3)
[Ni(dmpp) ₂]	2.1479(6)	2.1443(6)			
[Pt(dmpp) ₂]	2.2721(8)	2.2709(8)			

and 1.99 Å for [Ni(dmpp)₂(CH₃CN)]²⁺. In the former a disorder problem involving the acetonitrile ligand probably contributes to the long bond length. In [Ni(dppm)₂(CH₃CN)]²⁺ the Ni–N bond distance is 2.10 Å.^{22a} This would indicate that the Ni–N bond length is significantly shorter for an equatorially bound acetonitrile as compared to an axially bound acetonitrile. Both of the acetonitrile ligands are slightly bent at the N atom by 10–15°, presumably due to steric interactions for [Ni(dmpp)₂(CH₃CN)]²⁺ and packing forces for [Ni(dmpe)₂(CH₃CN)]²⁺.

Drawings of the two M(0) complexes Ni(dmpp)₂ and Pt(dmpp)₂ are shown in Figure 5. These two complexes are both slightly distorted tetrahedral complexes. The dihedral angle between the two planes defined by the phosphorus atoms of

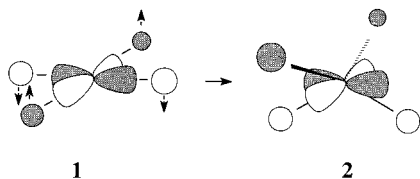
each diphosphine ligand and the metal are 87.4 and 89.7° for Ni(dmpp)₂ and Pt(dmpp)₂, respectively. For the Ni complex, the average Ni–P bond distance is 2.15 Å. For the Pt complex the average Pt–P bond distance is 2.27 Å. Although reduction generally results in a lengthening of metal–ligand bonds, these values are 0.06 Å shorter than the corresponding values of their Ni(II) and Pt(II) analogues. However, a similar bond shortening occurs during the reduction sequence [Ir(dppf)₂]⁺/[Ir(dppf)₂]/[Ir(dppf)₂]⁻.³⁰ These data suggest that bond shortening will generally occur upon reduction of square-planar d⁸ complexes to form tetrahedral d¹⁰ complexes.

(30) Longato, B.; Riello, L.; Bandoli, G.; Pilloni, G. *Inorg. Chem.* **1999**, *37*, 2818.

Discussion

As pointed out by Labinger, the transfer of a hydride ligand will almost always produce a coordinatively unsaturated species. This led him to conclude that measurement of hydricity for transition-metal hydrides would need to rely on more “phenomenological tests.”^{13a} However, there are stable 16-electron species such as the square-planar d⁸ transition-metal complexes. It was the stability of [M(diphosphine)₂]²⁺ complexes of Ni and Pt that suggested to us that [HM(diphosphine)₂]⁺ complexes might function as useful hydride donors for the reduction of metal carbonyl complexes.¹⁵ The objective of this work is to demonstrate a quantitative measure of the relative hydricity for [HM(diphosphine)₂]⁺ complexes and to delineate some of the features that determine their hydridic character.

Structural Studies. Diffraction studies of several of these complexes were performed to probe structure–activity relationships. The Ni(II) complexes can be isolated as either four- or five-coordinate species. The gross geometry of the five-coordinate complexes depends on the bite size of the diphosphine ligand. For [Ni(dmpe)₂(CH₃CN)]²⁺ a square-pyramidal geometry is observed with an apical acetonitrile, whereas [Ni(dmpp)₂(CH₃CN)]²⁺ is a trigonal bipyramid in which the acetonitrile ligand occupies an equatorial position. The small chelate bites observed for [Ni(dmpe)₂]²⁺ and [Ni(depe)₂]²⁺ produce nearly planar complexes. The larger chelate bites observed for [Ni(dmpp)₂]²⁺ and [Pt(dmpp)₂]²⁺ result in significant tetrahedral distortions. The LUMO of these complexes is shown for planar (**1**) and tetrahedrally distorted geometries (**2**).



The antibonding overlap between the metal d orbital and the ligand orbitals is decreased in **2** compared to **1**, and LUMO **2** is stabilized with respect to LUMO **1**, as described in detail in a previous publication.^{22a} This simple molecular orbital picture provides a useful approach to understanding the thermodynamic properties of the [M(diphosphine)₂]²⁺ complexes and their hydride analogues.

Dissociation of the acetonitrile ligands from the five-coordinate [Ni(diphosphine)₂(CH₃CN)]²⁺ complexes to produce four-coordinate complexes is facile, and the energy differences between the four- and five-coordinate complexes are small (1–3 kcal/mol). As a result of the small energy differences between the four- and five-coordinate species, the energetics of these five-coordinate complexes can be understood in terms of the corresponding four-coordinate complexes.

Both Ni(dmpp)₂ and Pt(dmpp)₂ have dihedral angles between the two planes defined by the diphosphine ligand and the metal of nearly 90°. This indicates that during reduction from [M(diphosphine)₂]²⁺ to M(diphosphine)₂ these metal complexes undergo a distortion from square-planar structures to tetrahedral structures. This twisting motion is larger for the Ni and Pt complexes with diphosphine ligands with small bite sizes because the M(II) complexes are more planar. Reduction is also accompanied by a contraction of the M–P bond lengths of approximately 0.06 Å.

Electrochemical Studies. The substituents on the diphosphine ligands, the nature of the metal, and the size of the chelate bite of the diphosphine ligand all have comparable effects on the

Table 6. Selected Bond Angles (deg)

[Ni(dmpe) ₂](PF ₆) ₂			
P(2)–Ni–P(1)	85.933(16)	P(2)–Ni–P(4)	177.613(18)
P(1)–Ni–P(4)	93.826(16)	P(2)–Ni–P(3)	93.998(16)
P(1)–Ni–P(3)	177.701(18)	P(4)–Ni–P(3)	86.338(16)
[Ni(depe) ₂](BF ₄) ₂			
P(2)–Ni–P(2A)	180.0	P(2)–Ni–P(1A)	95.222(14)
P(2)–Ni–P(1)	84.778(14)		
[Ni(dmpp) ₂](BF ₄) ₂			
P(1)–Ni–P(4)	99.926(18)	P(1)–Ni–P(3)	149.834(17)
P(1)–Ni–P(2)	89.18(3)	P(3)–Ni–P(2)	93.34(3)
P(4)–Ni–P(3)	93.851(19)	P(4)–Ni–P(2)	147.74(4)
[Pt(dmpp) ₂](PF ₆) ₂			
P(1)–Pt–P(2)	88.06(4)	P(1)–Pt–P(3)	171.62(5)
P(1)–Pt–P(4)	93.62(5)	P(2)–Pt–P(3)	91.29(4)
P(2)–Pt–P(4)	172.25(5)	P(4)–Pt–P(3)	88.14(5)
[Ni(dmpe) ₂ (CH ₃ CN)](PF ₆) ₂			
P(1)–Ni–P(4)	91.69(10)	P(1)–Ni–P(2)	85.21(8)
P(4)–Ni–P(2)	163.9(5)	P(1)–Ni–P(3)	162.5(5)
P(4)–Ni–P(3)	85.08(10)	P(2)–Ni–P(3)	93.14(10)
P(1)–Ni–N	99.1(3)	P(4)–Ni–N	97.4(5)
P(2)–Ni–N	98.7(3)	P(3)–Ni–N	98.4(4)
[Ni(dmpp) ₂ (CH ₃ CN)](BF ₄) ₂			
N–Ni–P(1)	82.55(10)	N–Ni–P(2)	127.74(10)
P(1)–Ni–P(2)	88.76(4)	N–Ni–P(3)	87.70(10)
P(1)–Ni–P(3)	169.91(4)	P(2)–Ni–P(3)	95.19(4)
N–Ni–P(4)	110.35(10)	P(1)–Ni–P(4)	96.20(4)
P(2)–Ni–P(4)	121.81(4)	P(3)–Ni–P(4)	89.61(4)
[Ni(dmpp) ₂]			
P(2)–Ni–P(2A)	113.41(4)	P(2)–Ni–P(1A)	115.41(2)
P(2)–Ni–P(1)	101.24(2)	P(1)–Ni–P(1A)	110.72(4)
[Pt(dmpp) ₂]			
P(2)–Pt–P(2A)	115.85(4)	P(2)–Pt–P(1A)	114.73(3)
P(2)–Pt–P(1)	99.75(3)	P(1)–Pt–P(1A)	112.82(4)

reduction potentials of the [M(diphosphine)₂]²⁺ complexes. It can be seen from Table 2 that the influence of the substituents on the redox potentials follows the expected order of electron-donating ability, Me > Et > Ph. Changing from a methyl to a phenyl substituent produces a 0.49 V difference between the reduction potential of [Pt(dmpe)₂]²⁺ and [Pt(dppe)₂]²⁺ and a 0.55 V shift for the average reduction potentials of the analogous Ni complexes. The reduction potentials for the Pt complexes are approximately 0.45 V more negative than the average of the Ni(II/I) and Ni(I/0) couples for the same ligand. The effect of the chelate bite size is somewhat different than changing the metal or the ligand substituents, because it has a significant effect on the potentials of the II/I couples but not on the potentials of the I/0 couples. The Ni(II/I) couple for [Ni(dmpp)₂]²⁺ is 0.5 V positive of the Ni(II/I) couple for [Ni(dmpe)₂]²⁺. Similarly the redox potential for the II/I couple of [Ni(dppp)₂]²⁺ (where dppp is 1,3-bis(diphenylphosphino)propane) is 0.54 V positive of that of [Ni(dppe)₂]²⁺ in dichloromethane.^{22a} However, the E_{1/2} values for the I/0 couples of [Ni(dppe)₂]²⁺ and [Ni(dppp)₂]²⁺ are nearly the same, and this is also true for [Ni(dmpe)₂]²⁺ and [Ni(dmpp)₂]²⁺. Comparison of the redox potentials of Pt(dmpe)₂ and Pt(dmpp)₂ shows that changing from a diphosphine ligand with a two-carbon backbone to one with a three-carbon backbone produces a change in the II/0 couple of approximately +0.25 V. This value is what would be expected if the Pt(II/I) couples shifted to more positive potentials by approximately 0.5 V and the potentials of the I/0 couples remained the same. As discussed above, the tetrahedral distortion observed for [M(diphosphine)₂]²⁺ complexes containing diphosphine ligands with large chelate bites leads to a lower energy of the LUMO by decreasing antibonding interactions. This results in more positive potentials for the II/I couples of

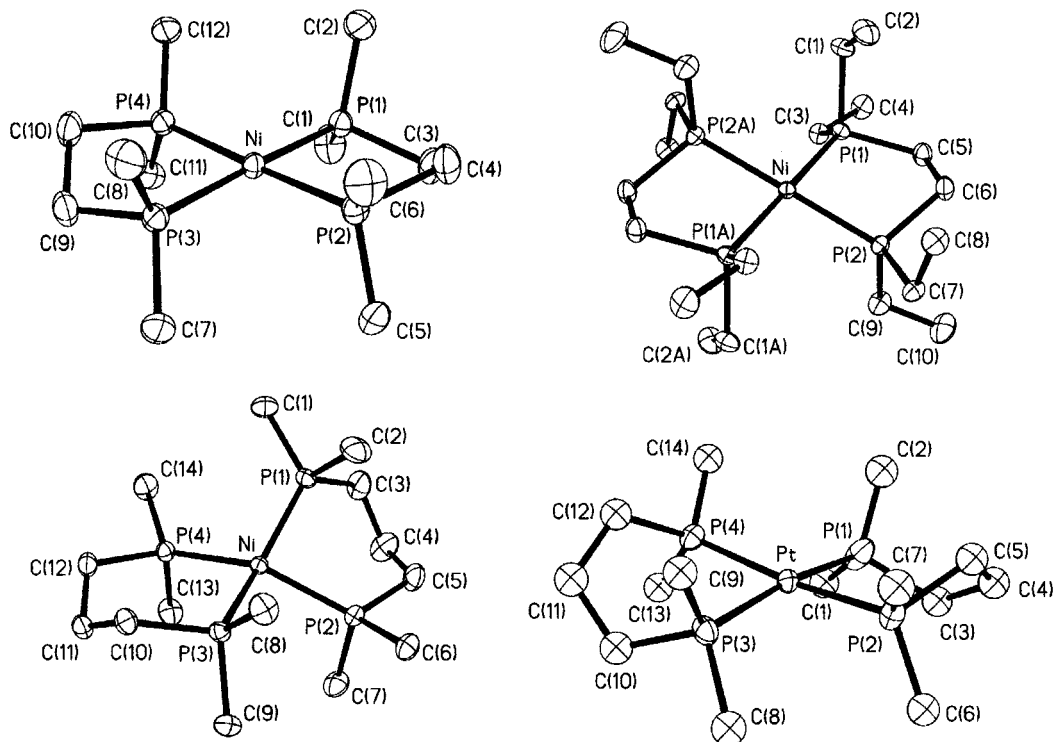


Figure 3. Drawings of $[\text{Ni}(\text{dmpe})_2]^{2+}$, $[\text{Ni}(\text{depe})_2]^{2+}$, $[\text{Ni}(\text{dmpp})_2]^{2+}$, and $[\text{Pt}(\text{dmpp})_2]^{2+}$ cations showing the atom-numbering schemes.

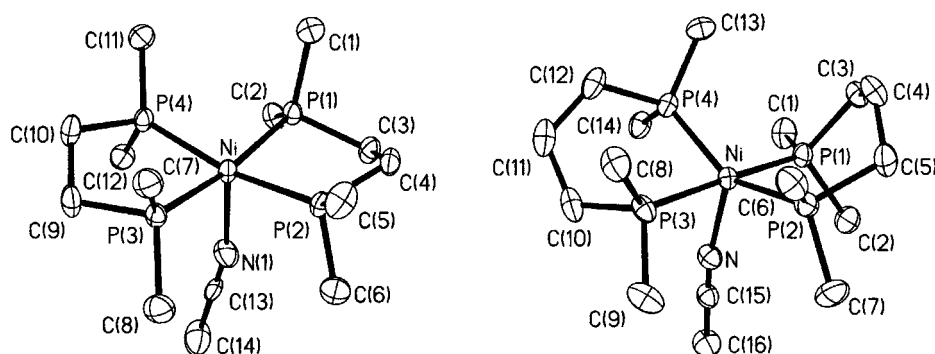


Figure 4. Drawings of $[\text{Ni}(\text{dmpe})_2(\text{CH}_3\text{CN})]^{2+}$ and $[\text{Ni}(\text{dmpp})_2(\text{CH}_3\text{CN})]^{2+}$ cations showing the atom-numbering schemes.

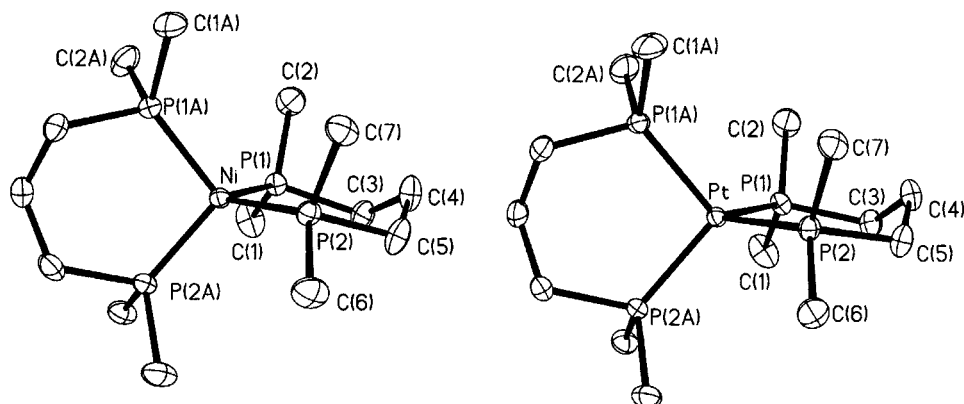


Figure 5. Drawings of $\text{Ni}(\text{dmpp})_2$ and $\text{Pt}(\text{dmpp})_2$ showing the atom-numbering schemes.

complexes containing diphosphine ligands with larger bite sizes. The potential of the I/O couple does not depend on the chelate bite size, because the Ni(I) and Pt(I) complexes are expected to have a nearly tetrahedral geometry.^{30,31}

The observation that chelate bite size has a significant effect on the II/I couple but not on the I/O couple has some interesting consequences. Large chelate bites can be used to stabilize the

M(I) oxidation state. For example, $[\text{Pd}(\text{dppx})_2]^+$ (where dppx is α,α' -bis(diphenylphosphino)-*o*-xylene) can be observed as a stable species, as discussed in a previous publication.^{22a} The stabilization of Pd(I) and Pt(I) species would suggest that radical type chemistry could play important roles for these complexes.

(31) Zotti, G.; Zecchini, S.; Pilloni, G. *J. Organomet. Chem.* **1983**, 246, 61.

A possible example of this radical chemistry is the reaction of [Pt(dmpe)₂]⁺ (produced by comproportionation of Pt(II) and Pt(0) complexes) with H₂ to form [HPt(dmpe)₂]⁺ in benzonitrile, which was described above. This reaction is more rapid for the dmpp analogue, as would be expected from a higher concentration of the M(I) species. Radical chemistry of [M(diphosphine)₂]⁺ complexes should be favored by large chelate bites, large substituents, and high temperatures.

Because the reductions of the [M(diphosphine)₂]²⁺ complexes produce large structural distortions, the role that entropy plays in determining the $E_{1/2}$ values could be significantly larger than that expected for complexes in which the structural changes are not so dramatic. However, the experimental $\Delta S^\circ_{\text{rc}}(\text{II}/0)$ values shown in Table 2 are in reasonable agreement with the values calculated using the method of Hupp and Weaver,^{25c} which are also shown in Table 2. The higher experimental values for $\Delta S^\circ_{\text{rc}}(\text{II}/\text{I})$ compared to the calculated values for the nickel complexes may be partly attributed to the loss of a nitrile ligand upon reduction, which would be expected to increase the entropy in addition to that associated with the change in charge. These results indicate that the structural distortions are not leading to abnormally large entropy contributions. Consequently, the order of the free energy changes and the enthalpy changes for these redox couples are the same, as shown in Table 2.

pK_a Measurements. In the pK_a measurements discussed above, all of the nickel and platinum complexes containing diphosphine ligands with methyl or ethyl substituents can be referenced back to a common organic base, tetramethylguanidine. Therefore, the relative free energies of proton transfer between the M(0) and M–H complexes for these complexes are unambiguously determined for these complexes in benzonitrile. Because the acidities of [HNi(dppe)₂]⁺ and [HPt(dppe)₂]⁺ are significantly different from those of the other complexes studied, pyridine and triethylamine, respectively, were used as bases. The factors which determine the pK_a values of the [HM(diphosphine)₂]⁺ complexes are, in order of decreasing importance: the substituents of the diphosphine ligands, the metal, and the chelate bite size of the diphosphine ligand. The pK_a values decrease by 5–10 pK_a units if the methyl substituents are replaced with phenyl substituents, by 3–8 units if Pt is replaced with Ni, and by 0.3–0.7 unit upon changing from a five- to a six-membered chelate ring.

The proton transfer between Pt and Ni complexes containing the same diphosphine ligands and between all of the Ni complexes likely proceeds via M–H–M' bridges.³² In the case of two different Pt complexes, the role of hydride exchange between two Pt metals is less clear. Reactions between [HPt(L)₂]⁺ and Pt(L')₂ complexes (where L and L' are two different diphosphine ligands) resulted in mixed [HPt(L)(L')]⁺ and Pt(L)(L') complexes. The exchange of diphosphine ligands permits the determination of pK_a values for platinum hydride complexes containing two different diphosphine ligands, but it is not clear whether the apparent hydride transfer involves the transfer of a hydride ligand, the transfer of diphosphine ligands, or both. Studies of the reactions of [HPt(L)₂]⁺ with [HPt(L')₂]⁺ and of Pt(L)₂ with Pt(L')₂ indicate that rapid diphosphine ligand scrambling reactions occur at room temperature for both Pt–H and Pt(0) species. Similar reactions are not observed for the analogous Ni(0) or Ni–H complexes at room temperature, and no diphosphine ligand scrambling is observed for either Ni(II) or Pt(II) complexes. We have interpreted these observations to

mean that the five-coordinate Pt–H and four-coordinate Pt(0) complexes undergo Pt–P bond cleavage reactions to form four-coordinate hydrides and three-coordinate Pt(0) intermediates. These unsaturated species can react with dangling phosphine ligands from a second intermediate to produce ligand exchange. Formation of analogous intermediates from the four-coordinate M(II) complexes is more difficult, and hence, scrambling is not observed in this case.

The temperature dependence of the equilibrium constant as measured by ³¹P NMR spectroscopy for the proton-transfer reaction between [HNi(dmpp)₂]⁺ and Ni(dmpe)₂ was studied to determine if there is a significant entropy contribution to this reaction. The measured value of ΔS° for this reaction is 6 ± 2 cal/(K mol). This result indicates that there are no large entropy contributions to the proton-transfer reactions resulting from differences in ring size of the chelating diphosphine ligands. Similar studies of the reactions between [HNi(depe)₂]⁺ and Ni(dmpe)₂ and between [HNi(dmpp)₂]⁺ and Ni(depe)₂ gave ΔS° values of -4 ± 2 and 5 ± 2 cal/(K mol), respectively. These data suggest that the ΔS° values for the proton-transfer reactions in our study are small.

Tilset and Parker have assumed that S° values of transition-metal hydrides and their corresponding radicals are the same, i.e., $S^\circ(\text{MH}^+) = S^\circ(\text{M}^+)$.^{7c} Substitution of $S^\circ(\text{M}^+)$ for $S^\circ(\text{MH}^+)$ for the entropy change associated with the proton exchange reaction (16) leads to the conclusion that $\Delta S^\circ_{\text{eq } 16}$ should equal the differences in the $\Delta S^\circ_{\text{rc}}(\text{I}/0)$ values observed in Table 2 for ML₂ and ML'₂ ($\Delta S^\circ_{\text{eq } 16} = \Delta \Delta S^\circ_{\text{rc}}(\text{I}/0)$). For the reaction of [Ni(dmpp)₂H]⁺ with Ni(depe)₂, the difference between the $\Delta S^\circ_{\text{rc}}(\text{I}/0)$ values is 5 ± 4 cal/(K mol) (see Table 2) compared to a ΔS° value of 5 ± 2 cal/(K mol) for the proton exchange reaction between [HNi(dmpp)₂]⁺ and Ni(depe)₂. This agreement suggests that S° values of M⁺ and MH⁺ complexes are the same in our study. Hopefully, variable-temperature measurements of proton exchange reactions and electron exchange reactions will be made on other systems so that the validity of the assumption that S° is the same for a transition-metal hydride (MH) and its radical (M[•]) may be tested more rigorously. It is important to establish that S° for MH and M[•] are the same, because the accuracy of the M–H bond dissociation energies derived from the thermochemical cycle shown in Scheme 1 depends on the validity of this assumption. However, if the M–H bond is strongly polarized to produce a dipole which collapses upon H[•] removal, it is not clear that the contribution to ΔS° resulting from the difference between MH and M[•] should be zero.

Hydride Transfer Potentials. The reaction of [HM(diphosphine)₂]⁺ complexes with [M(diphosphine)₂]²⁺ complexes resulted in a qualitative ordering of the hydride complexes in terms of their ability to donate hydride ligands. However, to obtain quantitative information, it was necessary to use the thermochemical cycle shown in Scheme 2. It can be seen from Table 3 that the order of $\Delta G^\circ_{\text{H}^-}$ values, or hydride transfer potentials, parallels the $E_{1/2}$ values for the II/0 couples, but the order does not follow the sequence of pK_a values. More electron-donating substituents increase the hydride donor potential with Me > Et > Ph. For example, [HNi(dmpe)₂]⁺ and [HPt(dmpe)₂]⁺ are approximately 14 kcal/mol better hydride donors than [HNi(dppe)₂]⁺ and [HPt(dppe)₂]⁺, respectively. For the same diphosphine ligand, platinum is a better hydride donor than Ni by 10–15 kcal/mol. A smaller chelate bite also appears to favor hydride transfer, because the hydride donor abilities of [HNi(dmpe)₂]⁺ and [HPt(dmpe)₂]⁺ are approximately 10 kcal/mol greater than those of [HNi(dmpp)₂]⁺ and [HPt(dmpp)₂]⁺, respectively. This is a direct result of the influence of the chelate bite size on the

(32) Numerous compounds containing M–H–M bridges are known: (a) Venanzi, L. M. *Coord. Chem. Rev.* **1982**, *43*, 251–274. (b) Knobler, C. B.; Kaesz, H. D.; Minghetti, G.; Bandini, A. L.; Banditelli, G.; Bonati, F. *Inorg. Chem.* **1983**, *22*, 2324–2331.

potential of the II/I redox couple. Of the complexes studied, the best hydride donor is $[\text{HPt}(\text{dmpe})_2]^+$, a third-row-metal complex containing a diphosphine ligand with a small chelate bite and electron-donating methyl groups.

Although a quantitative relationship could not be developed because of the slowness of the hydride transfer reaction, the observation that $[\text{HNi}(\text{depe})_2]^+$ and $[\text{HNi}(\text{dmpp})_2]^+$ can transfer a hydride ligand to *N*-benzylnicotinamide hexafluorophosphate indicates that the $[\text{HM}(\text{diphosphine})_2]^+$ complexes studied are more powerful hydride donors than most NADH analogues.

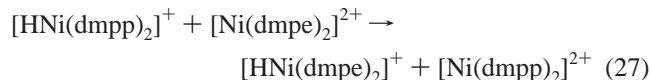
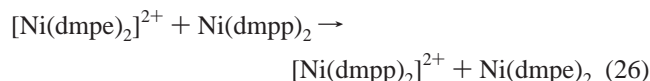
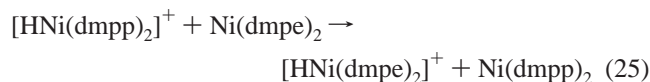
The $[\text{HM}(\text{diphosphine})_2]^+$ complexes in Table 3 are much more powerful hydride donors than the $\text{CpM}(\text{CO})_2(\text{L})\text{H}$ complexes ($\text{M} = \text{Mo}, \text{W}$) studied by Sarker and Bruno.¹² $[\text{HNi}(\text{dppe})_2]^+$, the poorest hydride donor in our study, is a stronger hydride donor by approximately 16 kcal/mol than $\text{CpMo}(\text{CO})_2(\text{PMe}_3)\text{H}$, the best hydride donor in the $\text{CpM}(\text{CO})_2(\text{L})\text{H}$ series; $[\text{HPt}(\text{dmpe})_2]^+$ is a stronger hydride donor by 40 kcal/mol. These data emphasize the important role of the stability of the unsaturated complexes that result from hydride transfer. For the $\text{CpM}(\text{CO})_2(\text{L})\text{H}$ complexes, hydride transfer is accompanied by coordination of the solvent, and the hydride transfer ability of these complexes should be strongly solvent dependent. For the $[\text{HM}(\text{diphosphine})_2]^+$ complexes, stable square-planar complexes are formed. The stability of the square-planar complexes is more important than the charge on the hydride complexes or the position of the transition metal in the Periodic Table.

Good hydride acceptors have the opposite characteristics of good hydride donors. From Table 3, it appears that $[\text{Ni}(\text{dppe})_2]^{2+}$ and $[\text{Ni}(\text{dmpp})_2]^{2+}$ should be the best hydride acceptors based on $\Delta G^\circ_{\text{H}^-}$. To evaluate the ability of these complexes to act as hydride acceptors, we studied the reaction of $[\text{Ni}(\text{dppe})_2]^{2+}$ and $[\text{Ni}(\text{dmpp})_2]^{2+}$ with hydrogen in dimethylformamide. It was observed that $[\text{Ni}(\text{dmpp})_2]^{2+}$ heterolytically cleaves hydrogen to form $[\text{HNi}(\text{dmpp})_2]^+$. In this case, the metal complex is a sufficiently good hydride acceptor that it can cleave the H–H bond, which illustrates the usefulness of the free energy data shown in Table 3 for suggesting feasible reactions. However, $[\text{Ni}(\text{dppe})_2]^{2+}$ does not react with hydrogen under the same conditions, which implies there is a kinetic constraint for this complex.

In previous studies, $[\text{Pd}(\text{tpE})(\text{DMF})]^{2+}$ (where tpE is bis-(3-(diethylphosphino)propyl)phenylphosphine and DMF is dimethylformamide) heterolytically cleaved hydrogen to form a hydride, but $[\text{Pd}(\text{etpE})(\text{DMF})]^{2+}$ (where etpE is bis(2-(diethylphosphino)ethyl)phenylphosphine) did not.³³ The only difference in these complexes is that tpE has a three-carbon chain backbone while etpE has a two-carbon chain backbone. This result also indicates the chelate bite size is important for heterolytic activation of hydrogen. We believe that this will prove to be a rather general phenomenon.

From the perspective of predicting the relative hydride donor or acceptor abilities of complexes in solution, the relative free energy of the hydride transfer reaction is the most important thermodynamic parameter. However, because the structural changes associated with hydride transfer are large (e.g., $[\text{HPt}(\text{depe})_2]^+$ is a distorted tetrahedron¹⁵ while $[\text{Pt}(\text{depe})_2]^{2+}$ is expected to be square planar on the basis of the structure of $[\text{Ni}(\text{depe})_2]^{2+}$), it is of interest to consider the entropy changes associated with the hydride transfer reactions. Ideally, the temperature dependence of the equilibrium constant for the transfer of the hydride ligand between $\text{M}'\text{H}^+$ and M^{2+} would provide this information. However, as discussed above, these

reactions proceed too far to completion to allow direct measurement of the equilibrium constants. An alternative approach, illustrated for the hydride exchange between $[\text{HNi}(\text{dmpp})_2]^+$ and $[\text{Ni}(\text{dmpe})_2]^{2+}$ in benzonitrile (reaction 27), is to use the entropy changes associated with reactions 25 and 26 to calculate the entropy change for reaction 27. $\Delta S^\circ_{\text{eq } 25}$ is the entropy associated



with proton exchange between $[\text{HNi}(\text{dmpp})_2]^+$ and $\text{Ni}(\text{dmpe})_2$, for which a value of 6 ± 2 cal/(K mol) was measured. $\Delta S^\circ_{\text{eq } 26}$ is the difference of $\Delta S^\circ_{\text{rc}}(\text{II}/0)$ values for the reaction of $\text{Ni}(\text{dmpp})_2$ with $[\text{Ni}(\text{dmpe})_2]^{2+}$ (2 ± 2 cal/K mol). The sum of ΔS° contributions from reactions 25 and 26 gives a value of 8 ± 4 cal/(K mol) for $\Delta S^\circ_{\text{eq } 27}$. This corresponds to a $T\Delta S$ contribution of 2.4 kcal/mol to the free energy of reaction 27 at room temperature. From Table 3 the free energy of reaction 27 is 11.6 kcal/mol, which gives an enthalpy contribution to reaction 27 of 14 kcal/mol. Therefore, $[\text{HNi}(\text{dmpe})_2]^+$ is a better hydride donor than $[\text{HNi}(\text{dmpp})_2]^+$ because of a larger enthalpic driving force. The entropic contribution at room temperature is small and opposite to the enthalpic contribution.

Using the same approach, ΔS° calculated for the hydride exchange between $[\text{HNi}(\text{depe})_2]^+$ and $[\text{Ni}(\text{dmpp})_2]^{2+}$ is 0 ± 4 cal/(K mol). Assuming S° for $\text{M}'\text{H}^+$ is equal to S° for M^+ and the same is true for $\text{M}'\text{H}^+$ and M'^+ , the entropy change associated with the hydride transfer between complexes $\text{M}'\text{H}^+$ and M^{2+} should be the difference in the $\Delta S^\circ_{\text{rc}}(\text{II}/\text{I})$ values associated with complexes M and M' . For the hydride exchange between $[\text{HNi}(\text{depe})_2]^+$ and $[\text{Ni}(\text{dmpp})_2]^{2+}$, this leads to a predicted ΔS° value of 0 compared to the experimental 0 ± 4 cal/(K mol). In conclusion, the entropy changes associated with the hydride transfer reactions in this study are small; consequently, the free energies for these reactions are determined primarily by enthalpy contributions.

A useful approach to understanding the features responsible for promoting the hydride transfer reaction is to view this reaction in a stepwise manner, in which the hydride ligand is first transferred without structural change followed by relaxation of the tetrahedral $\text{M}(\text{II})$ complex to a square-planar complex. This approach is frequently used for delineating the factors that promote hydrogen atom transfer.^{5a} If the hydride transfer step occurs without distortion, it will be favored by more basic substituents on the diphosphine ligands. Following hydride transfer, the tetrahedral $[\text{M}(\text{diphosphine})_2]^{2+}$ complexes will relax to square-planar structures. Because a tetrahedral $\text{Pt}(\text{II})$ complex is less stable than a tetrahedral $\text{Ni}(\text{II})$ complex, the driving force to form a square-planar platinum complex will be greater than for a nickel complex, and platinum complexes will be better hydride donors than nickel complexes. Similarly, complexes with large chelate bites will not be able to obtain a completely square-planar geometry. As a consequence, the driving force for hydride transfer will be less for complexes with large chelate bites.

(33) Wander, S. A.; Miedaner, A.; Noll, B. C.; Barkley, R. M.; DuBois, D. L. *Organometallics* **1996**, *15*, 3360–3373.

Summary and Conclusions

A thermochemical cycle has been used to measure the relative hydride donor abilities of a series of [HM(diphosphine)₂]⁺ complexes. On the basis of hydride transfer experiments, these complexes are better hydride donors than CpM(CO)₂(L)H complexes (where M = Mo, W and L = CO, PR₃) and most NADH analogues. The hydride donor abilities of the [HM(diphosphine)₂]⁺ complexes (M = Ni, Pt) in this study and the CpM'(CO)₂(L)H compounds (M' = Mo, W) studied by Sarker and Bruno span a range of 50 kcal/mol. For the [HM(diphosphine)₂]⁺ cations, the stability of the square-planar complexes formed on hydride transfer contributes more to the hydride donor ability than their position in the Periodic Table.

Structural differences between [HM(diphosphine)₂]⁺, M(diphosphine)₂, and [M(diphosphine)₂]²⁺ complexes are important for understanding differences in hydride donor ability. In this study, we have shown that electrochemical reduction of [M(diphosphine)₂]²⁺ to M(diphosphine)₂ results in a twisting of the diphosphine ligands about the metal to produce a tetrahedral structure with shorter M–P bonds. Protonation of the M(diphosphine)₂ complexes leads to [HM(diphosphine)₂]⁺ cations which have distorted tetrahedral M–P₄ structures and M–P bond distances comparable to [M(diphosphine)₂]²⁺ complexes (i.e., the bonds lengthen on protonation). Hydride transfer is accompanied by a tetrahedral to square-planar structural change without appreciable change in the M–P bond distance. Increasing the bite size of the diphosphine ligand of the [M(diphosphine)₂]²⁺ complexes produces a tetrahedral distortion of the square-planar complexes. This distortion makes these complexes easier to reduce, causes them to be better hydride acceptors, and stabilizes the +1 oxidation state. For [HM(diphosphine)₂]⁺ hydrides, the features favoring hydride donation are a third-row transition metal containing a diphosphine ligand with basic substituents and a small chelate bite.

Experimental Section

Physical Measurements and General Procedures. ¹H and ³¹P NMR spectra were recorded on a Varian Unity 300 MHz spectrometer at 299.95 and 121.42 MHz, respectively. ¹H chemical shifts are reported relative to tetramethylsilane using residual solvent protons as a secondary reference. ³¹P chemical shifts are reported relative to external phosphoric acid. For the ³¹P spectra of the platinum complexes, the spectra appear as a singlet flanked by satellites due to coupling to the ¹⁹⁵Pt (33.8% abundance) isotope. The chemical shift of the singlet is reported followed by ¹J_{Pt–P} obtained from the satellites. In the experiments where accurate, relative integrations of the ³¹P signals were needed, the repetition rate of the spectrometer was set to 11.96 s. Infrared spectra were recorded on a Nicolet 510P spectrometer as Nujol mulls. Absorption experiments were carried out on a Carey 5E UV–vis spectrometer. Elemental analyses were performed by Schwarzkopf Laboratories, Woodside, NY, or Galbraith Laboratories, Inc., Knoxville, TN. All syntheses were carried out using Schlenk and drybox techniques.

X-ray Diffraction Studies. Single-crystal X-ray data for eight complexes were collected at low temperature, ca. 150 K, on a Siemens SMART CCD diffractometer using Mo K α radiation ($\lambda = 0.71073$ Å). An arbitrary hemisphere of data to 0.68 Å resolution was collected for each sample. A full sphere was collected for [Ni(dmpp)₂(CH₃CN)](BF₄)₂, which crystallized in triclinic space group P1. Each data frame was 0.3° in ω ; frames were a correlated scan comprised of two exposures at half the total scan time. All data were corrected for Lorentz and polarization effects, as well as for absorption. Structure solution was by direct methods except for Ni(dmpp)₂, which was solved using the Patterson function. Anisotropic thermal parameters were refined for all non-hydrogen atoms. Details for specific compounds are given in the following paragraphs.

[Ni(dmpe)₂](PF₆)₂·CH₃NO₂. X-ray-quality crystals of [Ni(dmpe)₂](PF₆)₂ were grown from nitromethane/methanol. Data collection was at 150 K using 30 s scans. Structure solution and refinement proceeded normally. In addition to the Ni salt, the asymmetric unit contains one molecule of CH₃NO₂ disordered at two sites. One PF₆ anion exhibits rotational disorder.

[Ni(depe)₂](BF₄)₂·H₂O. Data collection was at 162 K using 30 s scans. Data beyond 0.75 Å resolution were discarded in the final refinement, due to weak scattering at high angle. Nickel is positioned on a crystallographic inversion center. The asymmetric unit is 0.5 Ni cation, one BF₄ anion, and 0.5 water. No disorder is present.

[Ni(dmpp)₂](BF₄)₂. Data collection was at 160 K using 10 s scans. The asymmetric unit consists of the Ni cation and two BF₄ anions. One dmpp ligand is disordered, showing inversion about the central carbon atom of the propane backbone.

[Pt(dmpp)₂](PF₆)₂·0.53CH₃CN·0.53CH₃OH. Crystals of [Pt(dmpp)₂](PF₆)₂ were grown from acetonitrile/methanol at –20 °C. Data collection was at 141 K using 30 s scans. The asymmetric unit is the Pt cation, two PF₆ anions, and 0.53 molecule each of methanol and acetonitrile. Both dmpp ligands are disordered, manifested as inversion about the central carbon of the propane backbone. One PF₆ displays rotational disorder.

[Ni(dmpe)₂(CH₃CN)](PF₆)₂·CH₃CN. Crystals of [Ni(dmpe)₂(CH₃CN)](PF₆)₂ were grown from acetonitrile/methanol at –20 °C. Data collection was at 170 K using 30 s scans. The asymmetric unit is comprised of the Ni cation, two PF₆ anions, and an additional molecule of acetonitrile. The Ni is out of the plane formed by the four P atoms. Ni is disordered across this plane. The two Ni sites are separated by 0.58 Å. A molecule of acetonitrile is present on either side of this plane, and each is within bonding distance (2.28 Å) when Ni is on the same side, and just out of distance (3.37 Å) when Ni is on the opposite side. Site occupancy is 0.59 for the major site and 0.41 for the minor site.

[Ni(dmpp)₂(CH₃CN)](BF₄)₂. Crystals of [Ni(dmpp)₂(CH₃CN)](BF₄)₂ were grown from acetonitrile/methanol at –20 °C. Data collection was at 169 K using 30 s scans over a full sphere of reciprocal space. The asymmetric unit contains two crystallographically independent sets of cations and anions. Disorder is present at the central carbon of a single propane backbone. No additional molecules are present. The system was examined for higher space group symmetry. No additional symmetry was found.

Ni(dmpp)₂. Crystals of Ni(dmpp)₂ were grown from toluene at –85 °C. Data collection was at 152 K using 90 s scans. The asymmetric unit is 0.5 molecule, with Ni on a 2-fold rotation axis. There is no disorder, and there are no additional molecules.

Pt(dmpp)₂. Crystals of Pt(dmpp)₂ were grown from toluene at –85 °C. Data collection was at 160 K using 30 s scans. The asymmetric unit is 0.5 molecule, with Pt on a 2-fold rotation axis. There is no disorder, and there are no additional molecules.

Electrochemical Studies. All electrochemical experiments were carried out under an atmosphere of N₂ in 0.3 M Bu₄NBF₄ in benzonitrile or 0.3 M Et₄NBF₄ in acetonitrile. Cyclic voltammetry experiments were carried out on a Cypress Systems computer-aided electrolysis system. The working electrode was a glassy-carbon disk (2 mm diameter), and the counter electrode was a glassy-carbon rod. A platinum wire immersed in a permethylferrocene/permethylferrocenium solution was used as a pseudoreference electrode to fix the potential. Ferrocene was used as an internal standard, and all potentials are referenced to the ferrocene/ferrocenium couple. Cell temperatures were maintained with a NESLAB RTE–110 refrigerated bath/circulator containing a 50/50 mixture of ethylene glycol and water.

Syntheses. 1,2-Bis(dimethylphosphino)ethane (dmpe), 1,2-bis(diethylphosphino)ethane (depe), bis(1,5-cyclooctadiene)nickel(0), and dichloro(1,5-cyclooctadiene)platinum(II) were purchased from Strem Chemical Co. and used without further purification. 1,3-Bis(dimethylphosphino)propane (dmpp) was purchased from Organometallics, Inc., and used without further purification. Benzonitrile, acetonitrile, ammonium hexafluorophosphate, 1,1,3,3-tetramethylguanidine, triethylamine, pyridine, tetrabutylammonium tetrafluoroborate, and tetraethylammonium tetrafluoroborate were purchased from Aldrich Chemical Co. and used as received. Tetrahydrofuran was purchased from Aldrich Chemical Co. and distilled over Na/benzophenone prior to use. [Ni(CH₃–

CN)₆(BF₄)₂ was prepared according to literature methods.³⁴ [Ni(dmpe)₂](BF₄)₂ and [Ni(depe)₂](BF₄)₂ were prepared by modified literature procedures,³⁵ which are similar to those of [Ni(dmpp)₂](BF₄)₂ discussed below. [Ni(dmpe)₂H](PF₆)₂, [Pt(dmpe)₂](PF₆)₂,³⁵ [Pt(depe)₂](PF₆)₂,³⁶ [Pt(dmpe)₂H](PF₆)₂, and [Pt(depe)₂H](PF₆)₂ were prepared according to the procedures in ref 15. Ni(dmpe)₂,³⁵ Ni(depe)₂,³⁷ and Pt(dmpe)₂³⁸ were prepared by modified literature procedures, and representative syntheses are described below. *N*-Benzylnicotinamide hexafluorophosphate was also prepared by a modified literature procedure.³⁹

[Ni(dmpp)₂](BF₄)₂. [Ni(CH₃CN)₆][BF₄]₂ (0.61 g, 1.22 mmol) was added as a solid to a solution of dmpp (0.41 g, 2.49 mmol) in degassed acetonitrile (100 mL) at room temperature. The solution was stirred at room temperature for 6 h, and the solvent was removed in vacuo to give a dark red solid. The solid was washed with methanol (3 × 5 mL) and dried overnight under vacuum to give the desired product in 88.0% yield. Anal. Calcd for C₁₄H₃₆B₂F₈NiP₄: C, 29.99; H, 6.47; P, 22.10. Found: C, 29.60; H, 6.71; P, 22.13. ¹H NMR (nitromethane-*d*₃): δ 1.76 (quintet, 24 H, ²J_{P-H} = 7.8 Hz, splitting 1.9 Hz, P(CH₃)₂), 2.05 (m, 8 H, PCH₂CH₂CH₂P), 2.23 (m, 4 H, PCH₂CH₂CH₂P). ³¹P NMR (nitromethane-*d*₃): δ -13.6 (s).

[Ni(depe)₂H](PF₆)₂. A solution of depe (1.05 g, 5.09 mmol) in THF (125 mL) was cooled to -78 °C, and Ni(COD)₂ (0.70 g, 2.54 mmol, COD = 1,5-cyclooctadiene) was added as a solid. The solution was warmed to room temperature and stirred for an additional 16 h to give a clear, yellow solution of Ni(depe)₂. Ammonium hexafluorophosphate (0.85 g, 5.21 mmol) in THF (50 mL) was added, which resulted in the formation of a precipitate. The volume was reduced to approximately 10 mL in vacuo, and the suspension was filtered. The resulting solid was washed with water (3 × 10 mL) followed by diethyl ether (3 × 10 mL) and dried overnight in vacuo to give the product in 93.5% yield. Anal. Calcd for C₂₀H₄₉F₆P₅Ni: C, 38.95; H, 8.01. Found: C, 39.16; H, 7.89. IR (Nujol): ν_{Ni-H} 1924 cm⁻¹. ¹H NMR (nitromethane-*d*₃): δ -14.2 (s, 1 H, Ni-H), 1.12 (m, 24 H, P(CH₂CH₃)₂), 1.71-1.91 (m, 24 H, PCH₂CH₂P), P(CH₂CH₃)₂). ³¹P NMR (nitromethane-*d*₃): δ 46.2 (s).

[Ni(dmpp)₂H](PF₆)₂. The complex was synthesized using a procedure similar to that for [Ni(depe)₂H](PF₆)₂ in 94.1% yield. Anal. Calcd for C₁₄H₃₇F₆P₅Ni: C, 31.55; H, 7.01. Found: C, 31.56; H, 7.00. IR (Nujol): ν_{Ni-H} 1940 cm⁻¹. ¹H NMR (nitromethane-*d*₃): δ -14.3 (s, 1 H, Ni-H), 1.43 (m, 24 H, P(CH₃)₂), 1.72 (m, 8 H, PCH₂CH₂CH₂P), 2.00 (m, 4 H, PCH₂CH₂CH₂P). ³¹P NMR (nitromethane-*d*₃): δ -15.7 (s).

Ni(dmpe)₂. A solution of dmpe (1.10 g, 7.33 mmol) in THF (50 mL) was cooled to -78 °C, and Ni(COD)₂ (1.01 g, 3.67 mmol) was added as a solid. The solution was warmed to room temperature and stirred for an additional 16 h to give a clear, yellow solution of Ni(dmpe)₂. The solvent was removed in vacuo, and the product was washed with acetonitrile (3 × 10 mL). The solid was then dried under vacuum overnight to give the product in 72.9% yield. The product can be sublimed under high vacuum at 110 °C. ¹H NMR (toluene-*d*₈): 1.24 (s, 24 H, P(CH₃)₂), 1.38 (m, 8 H, PCH₂CH₂P). ³¹P NMR (toluene-*d*₈): 15.0 (s).

Ni(depe)₂. The complex was synthesized using a procedure similar to that for Ni(dmpe)₂ in 78.7% yield. ¹H NMR (toluene-*d*₈): δ 1.02

(m, 24 H, P(CH₂CH₃)₂), 1.31 (m, 8 H, PCH₂CH₂P), 1.44 (m, 16 H, P(CH₂CH₃)₂). ³¹P NMR (toluene-*d*₈): δ 40.5 (s).

Ni(dmpp)₂. The complex was synthesized using a procedure similar to that for Ni(dmpe)₂ in 80.3% yield. The product can be sublimed under high vacuum at 110 °C. ¹H NMR (toluene-*d*₈): δ 1.10 (m, 24 H, P(CH₃)₂), 1.30 (m, 8 H, PCH₂CH₂CH₂P), 1.73 (m, 4 H, PCH₂CH₂CH₂P). ³¹P NMR (toluene-*d*₈): δ -19.9 (s).

[Pt(dmpp)₂](PF₆)₂. Pt(COD)Cl₂ (0.80 g, 2.14 mmol) was added as a solid to dmpp (0.71 g, 4.32 mmol) in acetonitrile (75 mL), and the resulting mixture was stirred at room temperature for 16 h. The solvent was removed in vacuo to give a white solid. The solid was dissolved in water (25 mL), and a solution of NH₄PF₆ (1.00 g, 6.13 mmol) in water (20 mL) was added, which resulted in the formation of a white precipitate. The precipitate was collected by filtration, washed with water (3 × 10 mL), and dried under vacuum to give the product in 91.2% yield. Anal. Calcd for C₁₄H₃₆F₁₂P₆Pt: C, 20.67; H, 4.46; P, 22.85. Found: C, 20.68; H, 5.02; P, 22.47. ¹H NMR (nitromethane-*d*₃): δ 1.90 (quintet, 24 H, ²J_{P-H} = 7.2 Hz, ³J_{Pt-H} = 27.3 Hz, P(CH₃)₂), 2.30 (m, 8 H, PCH₂CH₂CH₂P), 2.40 (m, 4 H, PCH₂CH₂CH₂P). ³¹P NMR (nitromethane-*d*₃): δ -29.6 (s, ¹J_{Pt-P} = 2079 Hz).

[Pt(dmpp)₂H](PF₆)₂. Sodium borohydride on basic alumina (1.16 g of material with 10% NaBH₄ content, 3.06 mmol) was added as a solid to a solution of [Pt(dmpp)₂](PF₆)₂ (1.00 g, 1.23 mmol) in acetonitrile (50 mL). The resulting mixture was stirred at room temperature overnight. The alumina was removed by filtration, and the solvent was removed from the filtrate by applying a vacuum. The solid that formed was washed with ethanol (3 × 5 mL) to remove excess sodium borohydride and dried overnight under vacuum to give the product in 72.1% yield. Anal. Calcd for C₁₄H₃₇F₆P₅Pt: C, 25.11; H, 5.57. Found: C, 25.25; H, 5.56. IR (Nujol): ν_{Pt-H} 2072 cm⁻¹. ¹H NMR (acetonitrile-*d*₃): δ -12.55 (quintet, 1 H, ¹J_{Pt-H} = 642 Hz, ²J_{P-H} = 29 Hz, Pt-H). ³¹P NMR (acetonitrile-*d*₃): δ -54.4 (s, ¹J_{Pt-P} = 2295 Hz).

Pt(dmpe)₂. Sodium naphthalenide (0.1 M) in THF was added dropwise to a suspension of [Pt(dmpe)₂](PF₆)₂ (0.96 g, 1.22 mmol) in THF (100 mL) until the green color of the sodium naphthalenide persisted. The solution was stirred at room temperature for 2 h, and the solvent was removed by applying a vacuum. The resulting solid was washed with acetonitrile (3 × 10 mL) and dried overnight under a vacuum to give the product in 87.0% yield. The product can be sublimed under high vacuum at 110 °C. Anal. Calcd for C₁₂H₃₂Pt: C, 29.10; H, 6.51. Found: C, 29.03; H, 6.77. ¹H NMR (toluene-*d*₈): δ 1.32 (m, 8 H, PCH₂CH₂P), 1.42 (m, 24 H, ³J_{Pt-H} = 22 Hz, P(CH₃)₂). ³¹P NMR (toluene-*d*₈): δ -12.6 (s, ¹J_{Pt-P} = 3714 Hz).

Pt(depe)₂. The complex was synthesized using a procedure similar to that for Pt(dmpe)₂ in 59.4% yield. ¹H NMR (toluene-*d*₈): δ 0.99 (m, 24 H, P(CH₂CH₃)₂), 1.24 (m, 8 H, PCH₂CH₂P), 1.46 (m, 16 H, P(CH₂CH₃)₂). ³¹P NMR (toluene-*d*₈): δ 21.5 (s, ¹J_{Pt-P} = 3614 Hz).

Pt(dmpp)₂. The complex was synthesized using a procedure similar to that for Pt(dmpe)₂ in 58.2% yield. The product can be sublimed under high vacuum at 110 °C. Anal. Calcd for C₁₄H₃₆Pt: C, 32.13; H, 6.93. Found: C, 32.16; H, 7.08. ¹H NMR (toluene-*d*₈): δ 1.47 (m, 24 H, ³J_{Pt-H} = 21 Hz, P(CH₃)₂), 1.53 (m, 8 H, PCH₂CH₂CH₂P), 1.87 (m, 4 H, PCH₂CH₂CH₂P). ³¹P NMR (toluene-*d*₈): δ -52.1 (s, ¹J_{Pt-P} = 3661 Hz).

Relative Hydride Transfer Potentials (Reaction 14). These reactions were performed by adding 20-30 mg of [M(L)₂]²⁺ (M = Ni, Pt; L = dmpe, depe, dmpp) and 1 equiv of [M(L)₂H]⁺ (M = Ni, Pt; L = dmpe, depe, dmpp) to NMR tubes in a drybox followed by 0.7 mL of CD₃CN. The solutions were allowed 24 h to reach equilibrium. The relative concentration of each species present was calculated by integration of the ³¹P NMR signals.

Relative Proton-Transfer Potentials (Reaction 16). These experiments were performed by preparing 1.4 × 10⁻² M solutions of the metal hydride and M(0) complexes in benzonitrile in a drybox. Various aliquots were then added to NMR tubes to give a constant volume of 0.7 mL. The mixtures were allowed 24 h to reach equilibrium, and the relative concentration of each species present was calculated by integration of the ³¹P NMR signals.

Equilibrium Constants for Diphosphine Ligand Transfer (Reactions 17 and 18). These experiments were performed by preparing 1.4 × 10⁻² M solutions of the platinum hydride and platinum(0) complexes

(34) Hathaway, B. J.; Holah, D. G.; Underhill, A. E. *J. Chem. Soc.* **1962**, 2444.

(35) (a) Hope, E. G.; Levason, W.; Powell, N. A. *Inorg. Chim. Acta* **1986**, *115*, 187. (b) von Kozelka, J.; Ludwig, W. *Helv. Chim. Acta* **1983**, *66*, 902. (c) Gulliver, D. J.; Levason, W.; Smith, K. G. *J. Chem. Soc., Dalton Trans.* **1981**, 2153.

(36) (a) Ittel, S. D. *Inorg. Synth.* **1990**, *28*, 98. (b) Ittel, S. D. *Inorg. Synth.* **1977**, *17*, 117. (c) Tolman, C. A.; Seidel, W. C.; Gosser, L. W. *J. Am. Chem. Soc.* **1974**, *96*, 53.

(37) (a) Mastrorilli, P.; Moro, G.; Nobile, C. F.; Latronico, M. *Inorg. Chim. Acta* **1992**, *192*, 183. (b) Gavero, G.; Frigo, A.; Turco, A. *Gazz. Chim. Ital.* **1974**, *104*, 869.

(38) (a) Chaloner, P. A.; Broadwood-Strong, G. T. L. *J. Chem. Soc., Dalton Trans.* **1996**, 1039. (b) Nuzzo, R. G.; McCarthy, T. J.; Whitesides, G. M. *Inorg. Chem.* **1981**, *20*, 1312.

(39) (a) Ostovic, D.; Han Lee, I.-S.; Roberts, R. M. G.; Kreevoy, M. M. *J. Org. Chem.* **1985**, *50*, 4206. (b) Karrer, P.; Stare, F. J. *Helv. Chim. Acta* **1937**, *20*, 418.

in benzonitrile in a drybox. Various aliquots of different hydride complexes (reaction 17) or different Pt(0) complexes (reaction 18) were then added to NMR tubes to give a constant volume of 0.7 mL. The mixtures were allowed 24 h to reach equilibrium, and the concentration of each species present was calculated by integration of the ³¹P NMR signals.

p*K*_a Measurements. These experiments were performed by preparing 1.4 × 10⁻² M samples of the metal hydride complexes in benzonitrile in a drybox. Various aliquots were then added to NMR tubes, followed by the appropriate base (tetramethylguanidine, pyridine, or triethylamine), to give a constant volume of 0.7 mL. The mixtures were equilibrated for 20 min, and the relative concentrations of the species present were calculated by integration of the ³¹P NMR signals.

Hydrogen Activation. These reactions were performed by dissolving 20–30 mg of [M(L)₂]²⁺ (M = Ni, Pt; L = dmpe, depe, dmpp) in dimethylformamide-*d*₇ (0.7 mL) and bubbling hydrogen through the solution. The reaction was monitored by ³¹P and ¹H NMR spectroscopy. Similar experiments were performed by dissolving equimolar amounts

of [M(diphosphine)₂]X₂ and M(diphosphine)₂ complexes in benzonitrile and bubbling hydrogen through the resulting solutions.

Acknowledgment. This work was supported by the U.S. Department of Energy, Office of Science, Chemical Sciences Division.

Supporting Information Available: Tables of crystal data, data collection parameters, structure solution and refinement, atomic coordinates and equivalent isotropic displacement parameters, bond lengths, bond angles, anisotropic thermal parameters, and hydrogen coordinates and isotropic displacement parameters for [Ni(dmpe)₂](PF₆)₂, [Ni(depe)₂](BF₄)₂, [Ni(dmpp)₂](BF₄)₂, [Pt(dmpp)₂](PF₆)₂, [Ni(dmpe)₂(CH₃CN)](PF₆)₂, [Ni(dmpp)₂(CH₃CN)](BF₄)₂, Ni(dmpp)₂, and Pt(dmpp)₂. This material is available free of charge via the Internet at <http://pubs.acs.org>.

JA991888Y